

AD-A242 429



2

**NAVAL POSTGRADUATE SCHOOL**  
**Monterey, California**

DTIC



**THESIS**

A CHARACTERIZATION OF UNDERWATER SOUND  
PRODUCED BY  
HEAVY PRECIPITATION

by

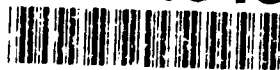
Lcdr. Chih-Lung Tan

December, 1990

Thesis Advisor: Jeffrey A. Nystuen

Approved for public release; distribution is unlimited.

91-15188



91 1106 033

Unclassified

Security Classification of this page

REPORT DOCUMENTATION PAGE			
1a Report Security Classification <b>Unclassified</b>		1b Restrictive Markings	
2a Security Classification Authority		3 Distribution Availability of Report <b>Approved for public release; distribution is unlimited.</b>	
2b Declassification/Downgrading Schedule		5 Monitoring Organization Report Number(s)	
4 Performing Organization Report Number(s)		7a Name of Monitoring Organization <b>Naval Postgraduate School</b>	
6a Name of Performing Organization <b>Naval Postgraduate School</b>	6b Office Symbol <b>68</b>	7b Address (city, state, and ZIP code) <b>Monterey, CA 93943-5000</b>	
6c Address (city, state, and ZIP code) <b>Monterey, CA 93943-5000</b>		9 Procurement Instrument Identification Number	
8a Name of Funding/Sponsoring Organization	8b Office Symbol (If Applicable)	10 Source of Funding Numbers	
8c Address (city, state, and ZIP code)		Program Element Number	Project No
11 Title (Include Security Classification) <b>A CHARACTERIZATION OF THE UNDERWATER SOUND PRODUCED BY HEAVY PRECIPITATION</b>		Task No	Work Unit Accession No
12 Personal Author(s) <b>CHIH-LUNG TAN</b>			
13a Type of Report <b>Master's Thesis</b>	13b Time Covered From To	14 Date of Report (year, month, day) <b>1990 December</b>	15 Page Count
16 Supplementary Notation <b>The views expressed in this thesis are those of the author and do not reflect the official policy or position of the Department of Defense or the U.S. Government.</b>			
17 Cosati Codes		18 Subject Terms (continue on reverse if necessary and identify by block number)	
Field	Group	Rainfall rate, Underwater sound Spectrum, Sonogram	
19 Abstract (continue on reverse if necessary and identify by block number)			
<p>An experiment by the Naval Postgraduate School and the National Data Buoy Center was performed in the Gulf of Mexico to investigate the underwater sound generated by heavy precipitation under a variety of conditons. During the first stage of the experiment, nine data sets were obtained with rainfall rates up to 300 mm/hr. The characteristic fifteen kilohertz peak in the underwater sound spectrum generated by small raindrops in light rain is absent during heavy rain. These data sets show a good correlation between rainfall rate and underwater sound levels, suggesting that acoustical measurement of rainfall rate at sea is possible. The correlation is best at lower frequencies (2-10 kHz). At higher frequencies (12-22 kHz) low spectral levels are observed in conditions of high wind (&gt; 10 m/s), presumably due to sound absorption by ambient bubble clouds from breaking waves. At very high rainfall rates (&gt;200 mm/hr), low levels at higher frequencies are also observed suggesting that the rain itself is capable of producing large populations of bubbles which absorb the sound radiated from the surface.</p>			
20 Distribution/Availability of Abstract		21 Abstract Security Classification	
<input checked="" type="checkbox"/> unclassified/unlimited <input type="checkbox"/> same as report <input type="checkbox"/> DTIC users		<b>Unclassified</b>	
22a Name of Responsible Individual <b>Jeffrey A. Nystuen</b>		22b Telephone (Include Area code) <b>(408) 646-2917</b>	22c Office Symbol <b>OC/NY</b>

DD FORM 1473, 84 MAR

83 APR edition may be used until exhausted

security classification of this page

All other editions are obsolete

Unclassified

Approved for public release; distribution is unlimited.

A CHARACTERIZATION OF UNDERWATER SOUND  
PRODUCED BY  
HEAVY PRECIPITATION

by

Chih-Lung Tan  
Lieutenant Commander, Republic of China Navy  
B.S., Chinese Naval Academy

Submitted in partial fulfillment  
of the requirements for the degree of

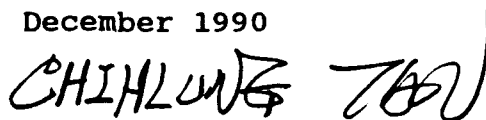
MASTER OF SCIENCE IN PHYSICAL OCEANOGRAPHY

from the

NAVAL POSTGRADUATE SCHOOL

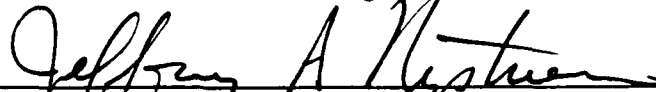
December 1990

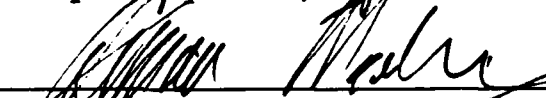
Author:

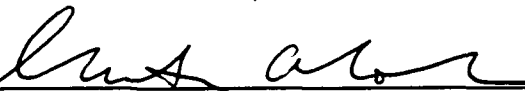


Chih-Lung Tan

Approved by:

  
Jeffrey A. Nystuen, Thesis Advisor

  
Herman Medwin, Second Reader

  
Curtis A. Collins, Chairman  
Department of Oceanography

**ABSTRACT**

An experiment by the Naval Postgraduate School and the National Data Buoy Center was performed in the Gulf of Mexico to investigate the underwater sound generated by heavy precipitation under a variety of conditions. During the first stage of the experiment, nine data sets were obtained with rainfall rates up to 300 mm/hr. The characteristic fifteen kilohertz peak in the underwater sound spectrum generated by small raindrops in light rain is absent during heavy rain. These data sets show a good correlation between rainfall rate and underwater sound levels, suggesting that acoustical measurement of rainfall rate at sea is possible. The correlation is best at lower frequencies (2-10 kHz). At higher frequencies (12-22 kHz) low spectral levels are observed in conditions of high wind (>10 m/s), presumably due to sound absorption by ambient bubble clouds from breaking waves. At very high rainfall rates (>200 mm/hr), low levels at higher frequencies are also observed suggesting that the rain itself is capable of producing large populations of bubbles which absorb the sound radiated from the surface.



Accession No.	
NTIS UNSOL	<input checked="" type="checkbox"/>
DTIC TAB	<input type="checkbox"/>
Unannounced	<input type="checkbox"/>
Justification	
By	
Distribution/	
Availability Codes	
Dist	Avail and/or special
A-1	

## TABLE OF CONTENTS

I. INTRODUCTION . . . . .	1
II. EXPERIMENTAL SETUP AND DATA ACQUISITION . . . . .	12
A. EXPERIMENTAL SETUP . . . . .	12
B. DATA ACQUISITION . . . . .	15
1. ACOUSTICAL RECORDING . . . . .	15
2. ENVIRONMENTAL DATA . . . . .	17
a. OPTICAL RAIN GAUGE . . . . .	17
b. RAIN ACCUMULATION SENSOR . . . . .	17
c. WIND SPEED SENSOR . . . . .	17
d. WAVE DATA . . . . .	17
e. NATIONAL WEATHER SERVICE RADAR DATA . . . . .	18
C. DATA PROCESSING . . . . .	18
III. DATA ANALYSIS . . . . .	27
A. PREDEPLOYMENT OBSERVATIONS . . . . .	27
B. UNDERWATER SOUND SPECTRUM WITH NO RAIN . . . . .	32
C. SOUND SPECTRA RECORDED UNDER CONDITIONS OF CONSTANT RAINFALL RATE WITH DIFFERENT WIND SPEEDS . . . . .	33
D. SOUND SPECTRA RECORDED UNDER CONDITIONS OF CONSTANT WIND SPEED WITH DIFFERENT RAINFALL RATES . . . . .	36
E. VERY HIGH RAINFALL RATES . . . . .	39

F. CORRELATION COEFFICIENTS FOR AMBIENT SOUND AND RAINFALL RATE . . . . .	43
IV. SUMMARY AND DISCUSSION . . . . .	51
V. CONCLUSIONS AND RECOMMENDATIONS . . . . .	54
LIST OF REFERENCES . . . . .	55
INITIAL DISTRIBUTION LIST . . . . .	58

**LIST OF TABLES**

Table I. Environmental conditions of the four different cases with steady winds. . . . .	43
Table II. Summary of correlation coefficients in four different cases. . . . .	50

## LIST OF FIGURES

Figure 1. Spectral densities of ocean noises . . . . .	3
Figure 2. The spectral level of ambient noise under low rainfall rate and different wind speeds . . . . .	4
Figure 3. Acoustic pressure of an impact and a bubble .	5
Figure 4. Regions of regular bubble creation . . . . .	7
Figure 5. The prediction of the effect of wind on the underwater sound generated by light rain . . . . .	8
Figure 6. Typical raindrop size distributions . . . . .	10
Figure 7. The location of Ocean Test Platform . . . . .	12
Figure 8. The Ocean Test Platform . . . . .	13
Figure 9. The OTP mooring design . . . . .	14
Figure 10. Control diagram of data acquisition . . . . .	15
Figure 11. The sensitivity curve of the hydrophone . .	19
Figure 12. Sound level spectrum from heavy rain . . . . .	20
Figure 13. Sonogram of the underwater sound caused by rainfall . . . . .	21
Figure 14. Block diagram of data processing . . . . .	22
Figure 15. Sonogram for three splashes by large raindrops . . . . .	24
Figure 16. Sound spectrum caused by a drop splash . . .	26
Figure 17. Spectrum of sound under light rain, light wind conditions . . . . .	27

Figure 18. A 580 ms sonogram of a light rain under light wind conditions . . . . .	28
Figure 19. Histogram of the resonance frequencies of bubbles generated by small drops . . . . .	29
Figure 20. Spectral level of the underwater sound caused by a light rain with large drops falling onto the canal . . . . .	30
Figure 21. Sonogram (290 ms) of underwater sound when there are larger drops in a light rain . . . . .	31
Figure 22. Sonogram (400 seconds) from the canal . . . . .	32
Figure 23. The intensity difference of spectras . . . . .	33
Figure 24. The spectral levels at 5 kHz and 21 kHz during constant 3.2 m/s wind . . . . .	34
Figure 25. The underwater sound spectra during 8 mm/hr rainfall rate with two different wind speeds . . . . .	35
Figure 26. The underwater sound spectrum during 15 mm/hr rainfall rate with two different wind speeds . . . . .	37
Figure 27. The underwater sound spectra when wind speed equals 5.5 m/s with two different rainfall rates . . . . .	38
Figure 28. The underwater sound spectra when wind speed equals 6.0 m/s with two different rainfall rates . . . . .	40
Figure 29. The underwater sound spectra when wind speed equals 3.5 m/s with two different rainfall rates . . . . .	41
Figure 30. The spectral levels of four different rainfall rates . . . . .	42

Figure 31. Correlation coefficients between rainfall rate and underwater sound spectrum on August 24 . . . .	45
Figure 32. Correlation coefficients between rainfall rate and underwater sound spectrum on August 27 . . . .	46
Figure 33. Correlation coefficients between rainfall rate and underwater sound spectrum on August 20 . . . .	48
Figure 34. Correlation coefficients between rainfall rate and underwater sound spectrum on August 30 . . . .	49
Figure 35. Comparison of rainfall rates and the sound spectral levels at 2 kHz . . . . .	52

### ACKNOWLEDGEMENTS

I wish to express gratitude and thanks to my advisor Dr. Jeffrey A. Nystuen, for his time, interest, and mostly, patience and encouragement during the preparation of this thesis. A special thanks to Dr. Herman Medwin for his expert guidance of this thesis, also to Mr. Timothy P. Stanton to help me modify the computer program of color waterfall sonogram. Also thanks to Mr. Mike Cook for his help during data processing.

Finally, and most certainly, I give my deepest love and gratitude to my wife Yanrong, for her comprehension, patience and love which made the completion of this thesis possible.

## I. INTRODUCTION

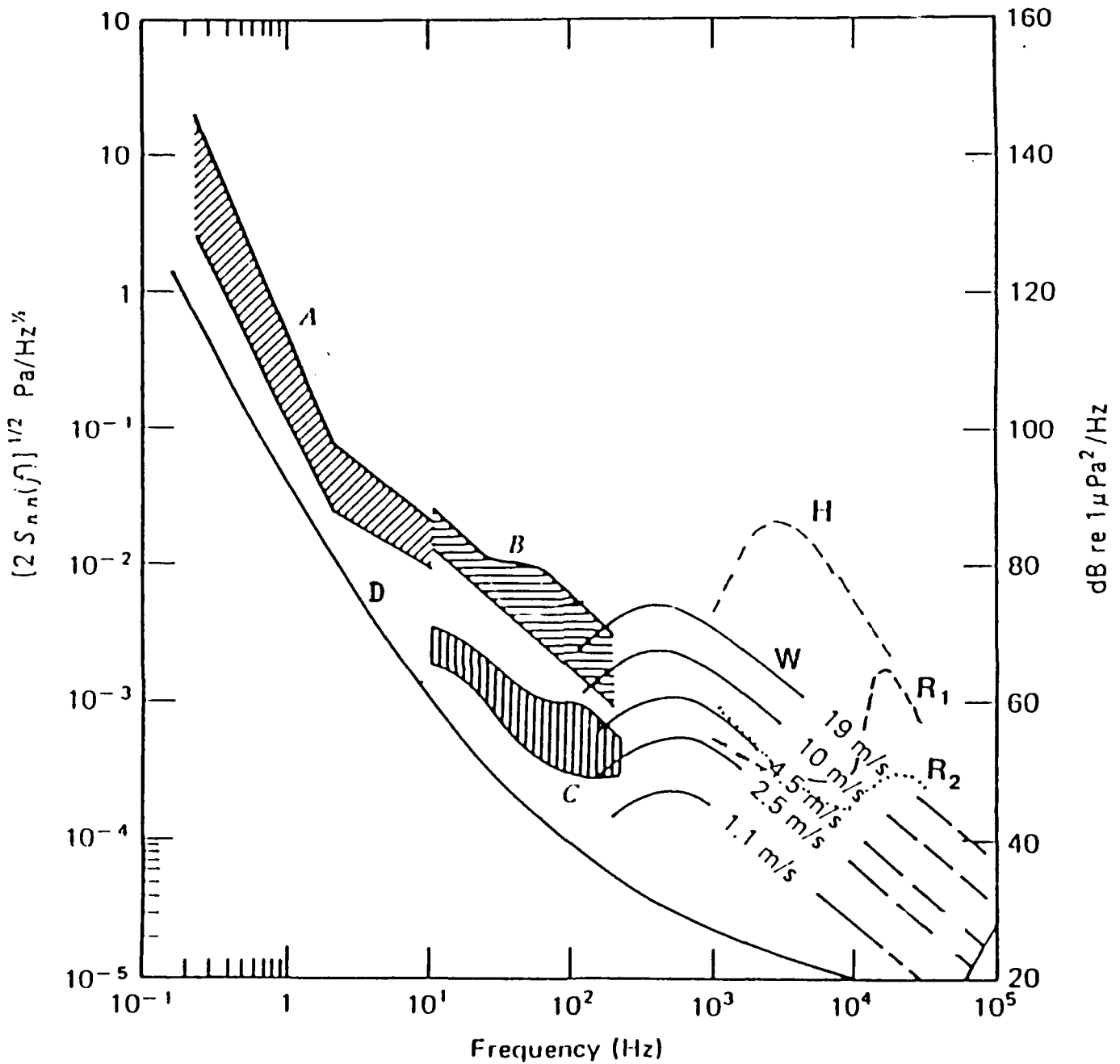
Precipitation is an important component of the coupled atmosphere/ocean climate system. In particular, good measurements of precipitation are needed to understand the heat balance processes. Over land, precipitation has traditionally been measured with simple rain gauges. However at sea, rain gauges are unreliable and, at present, there is no satisfactory self-contained rainfall sensor. All conventional designs are unreliable when mounted on unstable platforms (buoys or ships), and are subject to uncertainties caused by deformation of the air flow over large structures (e.g. oil platforms) or moving vessels. Some satellite techniques have been proposed to measure oceanic precipitation, but all of these methods lack independent surface verification.

Rainfall measurement using the underwater sound produced by the precipitation has received attention in the past few years. This development is important to weather forecasters and oceanographers because it potentially permits the detection and measurement of rain over the oceans by remote (buoyed or bottom-mounted) acoustic sensors. The technique used to monitor precipitation is simply to listen to the sound generated. Since the sound generation mechanisms are unique (different from wind), the spectral character of the observed

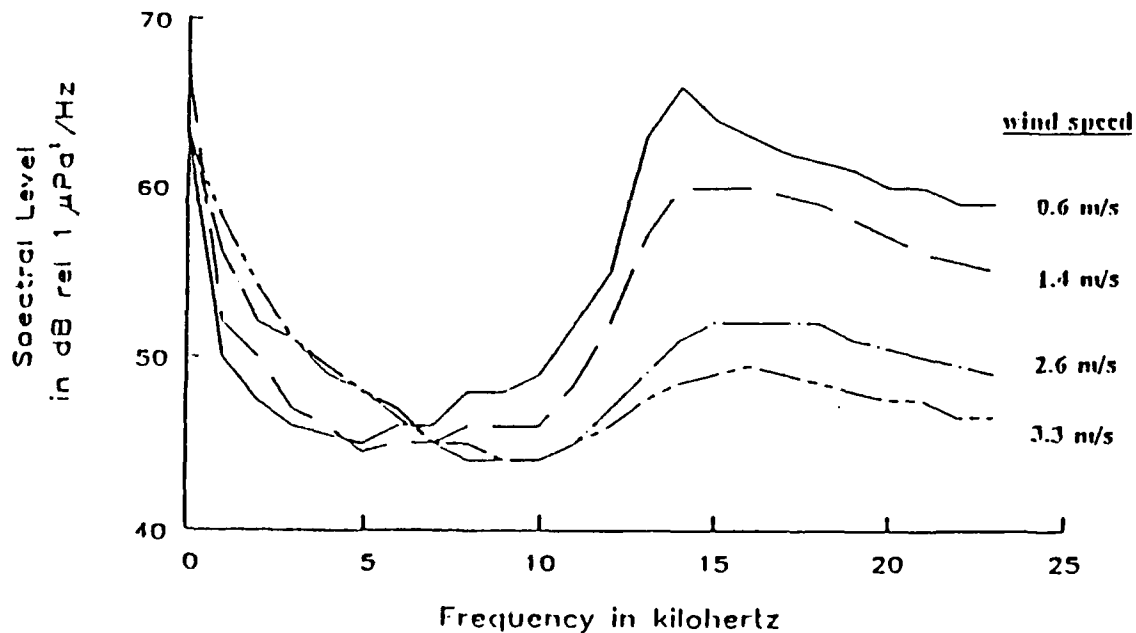
sound can be used to measure precipitation. However, a satisfactory algorithm to predict rainfall rate by analysing underwater sound generated by rain has not been achieved. This is because the influence of different air/sea conditions (wind, waves, etc.) on the rain-generated sound spectrum is not yet fully understood.

Figure 1 shows a generalized diagram of ambient sound in the ocean over a wide range of frequencies. Precipitation, rain in particular, is shown as a noise source in the frequency range (1-30 kHz). It has a distinctive shape which should allow it to be separated from wind noise, the other dominant sound source at these frequencies. The wind generated noise is thought to be due to bubbles generated by breaking waves (Knudsen et al., 1948; Farmer and Vagle, 1988; Medwin and Beaky, 1989). Ambient noise at 4.3, 8, and 14.5 kHz has been shown to be highly correlated with wind speed (Farmer and Lemon, 1984; Evans et al., 1984; Vagle et al., 1990) and results in a logarithmic fit between ambient noise and wind speed over the range of 0 - 12 m/s. At higher wind speeds (over 10 m/s), a subsurface bubble layer forms and attenuates the higher frequencies ( $\geq 10$  kHz) of surface generated noise (Farmer and Lemon, 1984; Farmer and Vagle, 1988).

The sound generated by light rain, containing only drops smaller than 1.5 mm in diameter, has also been studied extensively. In the absence of wind, a sharp peak in the underwater sound spectrum is observed at approximately 14 kHz



**Figure 1.** Spectral densities of ocean noises. D:the empirical minimum prevailing noise at sea. A:seismic, B:ships, C:quiet lake, H:hail, W:wind noise at different speeds, R<sub>1</sub>:rain with 0.6 m/s wind, R<sub>2</sub>:rain with 2.6 m/s wind (Clay and Medwin, 1977).



**Figure 2.** The spectral level of ambient noise under low rainfall rate and different wind speeds (Nystuen and Farmer 1987).

(Figure 2) (Nystuen and Farmer, 1987). Raindrops are known to produce underwater sound from the initial impact and, subsequently, from a bubble created by the drop splash. If a bubble occurs, its sound dominates the sound field. Figure 3 obtained by Kurgan (1989) (see Medwin et al. 1990) shows the sound pressure from a typical impact and the bubble created by a 0.83 mm diameter drop. The impact is a short single cycle pulse, so the spectral signature is a broadband peak. The bubble produces a damped oscillation with about 20 cycles and therefore the spectral signature of an individual bubble is a

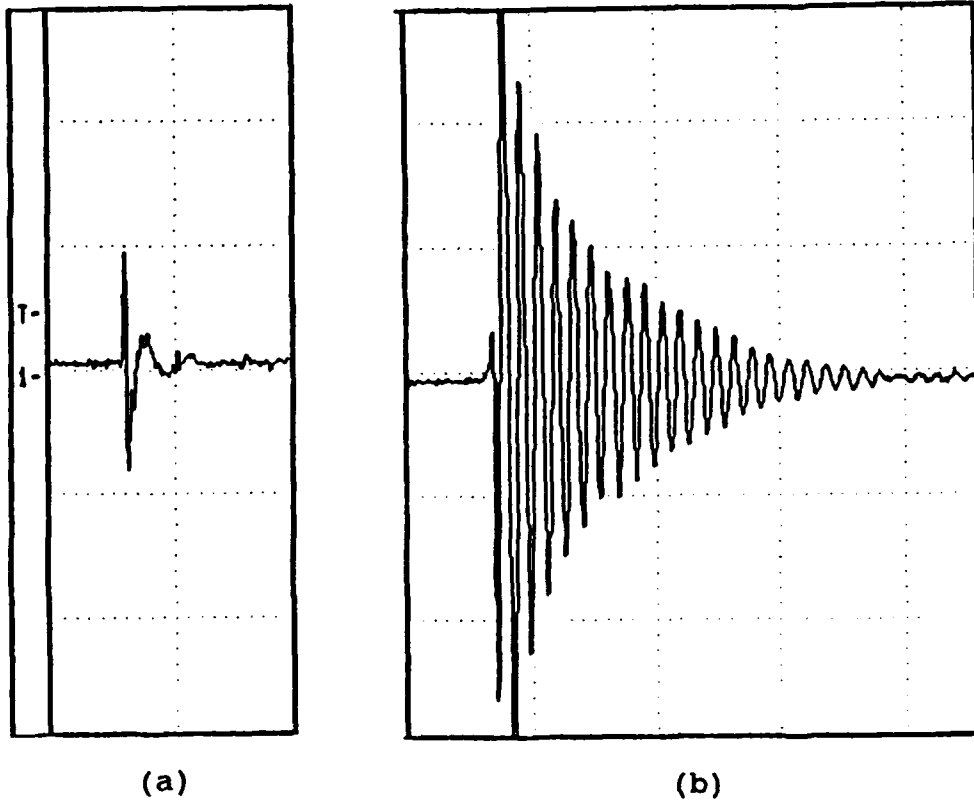


**Figure 3.** Acoustic pressure of: (a) an impact and (b) a bubble created by an 0.83 mm diameter water drop falling perpendicular to the surface. The time scale is 400  $\mu$ s per division and 30 ms occurs between the impact and the bubble (Kurgen, 1989).

narrow band peak centered at the resonance frequency of the bubble. The resonance frequency of a bubble depends on its size and is given by:

$$f_R = \frac{1}{2\pi a} \sqrt{\frac{3\gamma P_A}{\rho}} \quad (1)$$

where  $f_r$  is the resonance frequency,  $a$  is the radius of the drop,  $P_A$  is the ambient pressure and  $\gamma$  is the ratio of specific heats of the bubble gas (for air  $\gamma=1.4$ ).

The sound energy of the bubble was 200 times larger than the acoustic energy associated with the impact. Therefore, if every drop splash generates a bubble, the sound from the bubbles will dominate the radiating acoustic field completely. However, not all splashes generate bubbles in real rain. Because bubble production is a function of drop size and is influenced by wind and surface conditions. Understanding the relationship between different rainfall rates (drop sizes), wind speeds and the sound spectrum is a challenging problem which must be solved before an accurate acoustical estimation of rainfall rate can be achieved.

Laboratory experiments of Crum and Pumphrey (1989) identified a bubble entrainment mechanism for drop splashes which occurs in a narrowly defined size and impact velocity range (Figure 4). Drops occurring in this size and impact velocity range have a high probability of entraining bubbles (nearly 100%) at perpendicular incidence. The important region of this mechanism for sound generation by natural rainfall is the intersection of the entrainment region with the terminal velocity curve. Drops of the size 0.8-1.0 mm diameter entrain bubbles. The size of the entrained bubbles causes them to resonate at 14 kHz. This drop size range is always present in rain and explains why the 14-kHz peak is so ubiquitous and

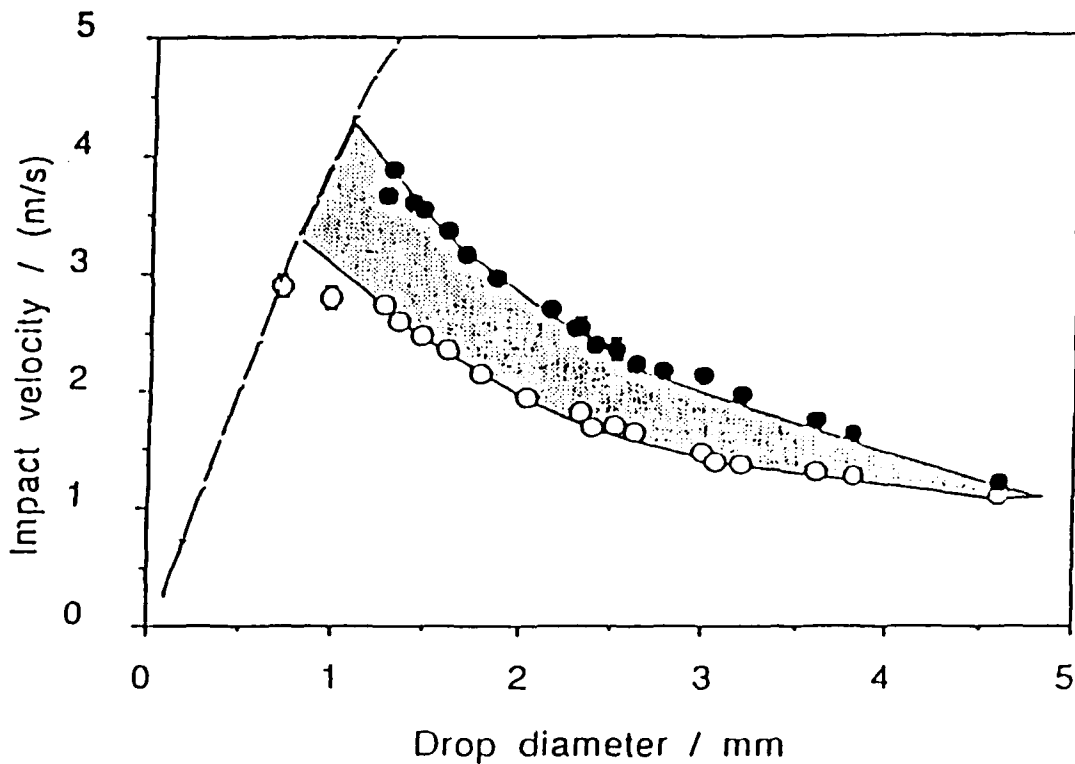


**Figure 4.** Regions of regular bubble creation. The shaded area shows the regular bubble creation area as a function of drop size and impact velocity (Crum and Pumphrey, 1989). The curve on the left is the terminal velocity for free falling drops in still air.

well defined.

The spectral peak at 14 kHz is observed under conditions of light rain (less than 4 mm/hr) and low wind speeds (less than 1 m/s). As conditions change, both the level and shape of the spectral peak change. Under constant wind conditions, spectral levels due to rain appear to be proportional to rainfall rate which suggests that the method of measuring rainfall rate acoustically will work. Scrimger et al. (1989)

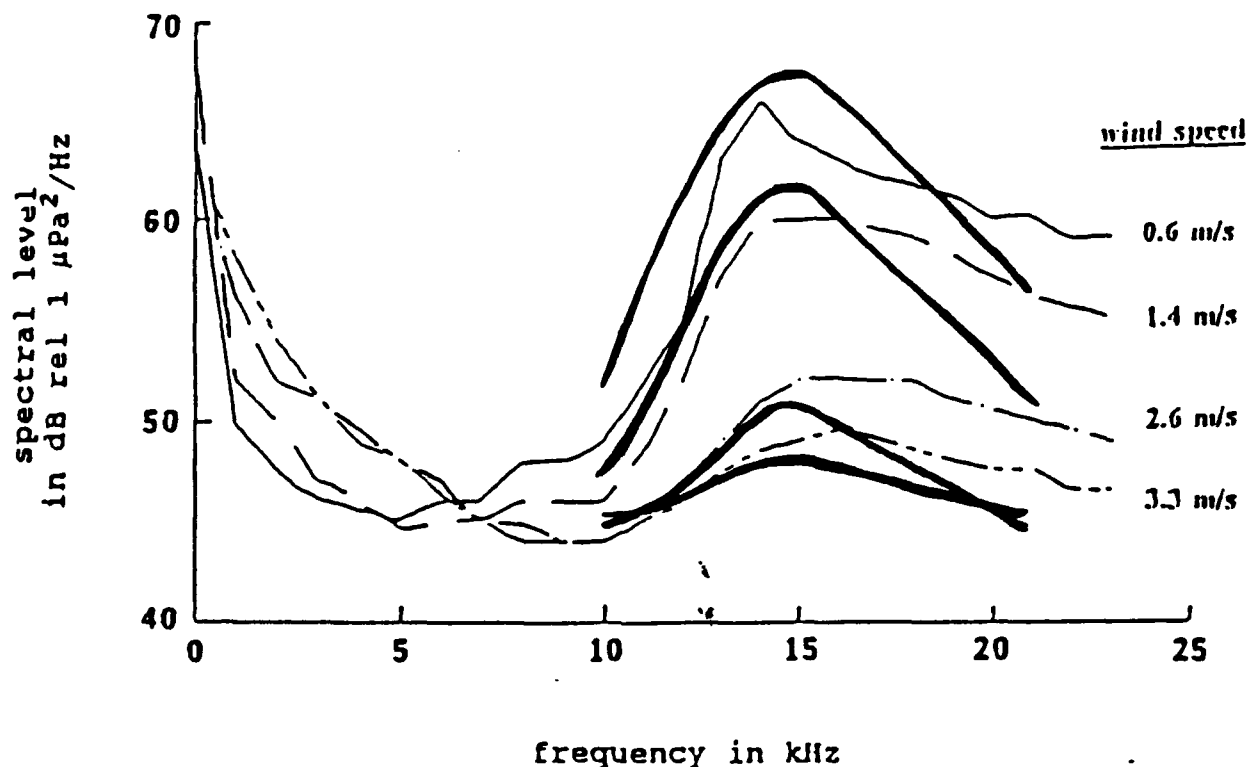


Figure 5. The prediction of the effect of wind on the underwater sound generated by light rain (heavy lines) superimposed onto field observations (light and dashed lines) (Nystuen, 1990).

suggest that spectral level shows a logarithmic dependence on rain rate, increasing 4 dB for each doubling of rain rate. When wind is present, the spectral peak shifts to a higher frequency and the spectral levels are depressed (Nystuen and Farmer, 1987). This was initially explained as a modification of the impact mechanism for sound generation. However this has recently been attributed to the suppression of the bubble entrainment mechanism for the small raindrops (Nystuen, 1990).

The bubble entrainment mechanism identified by Crum and Pumphrey is apparently very sensitive to the incident angle of the raindrop impact (Medwin et al., 1990). Wind blows the raindrops horizontally, causing them to strike obliquely. The wind also roughens the surface, producing a distribution of impact angles. Together these influences reduce the probability that a bubble will be entrained. For a wind of only 3.3 m/s, the probability that 0.8-1.0 mm drops entrain bubbles has dropped from 100% at normal incidence to 0.1% (Nystuen, 1990). Figure 5 shows the predicted effect together with observations.

From the point of view of measuring rainfall rate, rainfall rate is the volume of rainwater falling per unit time per unit area and is defined as:

$$RR = A \int_{d=200\mu m}^{d=5mm} DSD * V_t * (\pi * \frac{d^3}{6}) dd \quad (2)$$

where RR is rainfall rate (mm/hr), A is unit conversion constant (m<sup>2</sup>/mm<sup>2</sup>), DSD is the drop size distribution (#/m<sup>3</sup> mm), V<sub>t</sub> is terminal velocity (m/s), and d is drop diameter (mm). The terminal velocity is approximately proportional to d<sup>1/2</sup> and so RR is the d<sup>7/2</sup>th moment of the DSD. This means that the presence of large drops, not small ones, is better correlated with rainfall rate. Figure 6 shows the measured drop size distribution at Clinton Lake, IL. during a variety of rainfall rates. Note that while an increase in rainfall rate increases

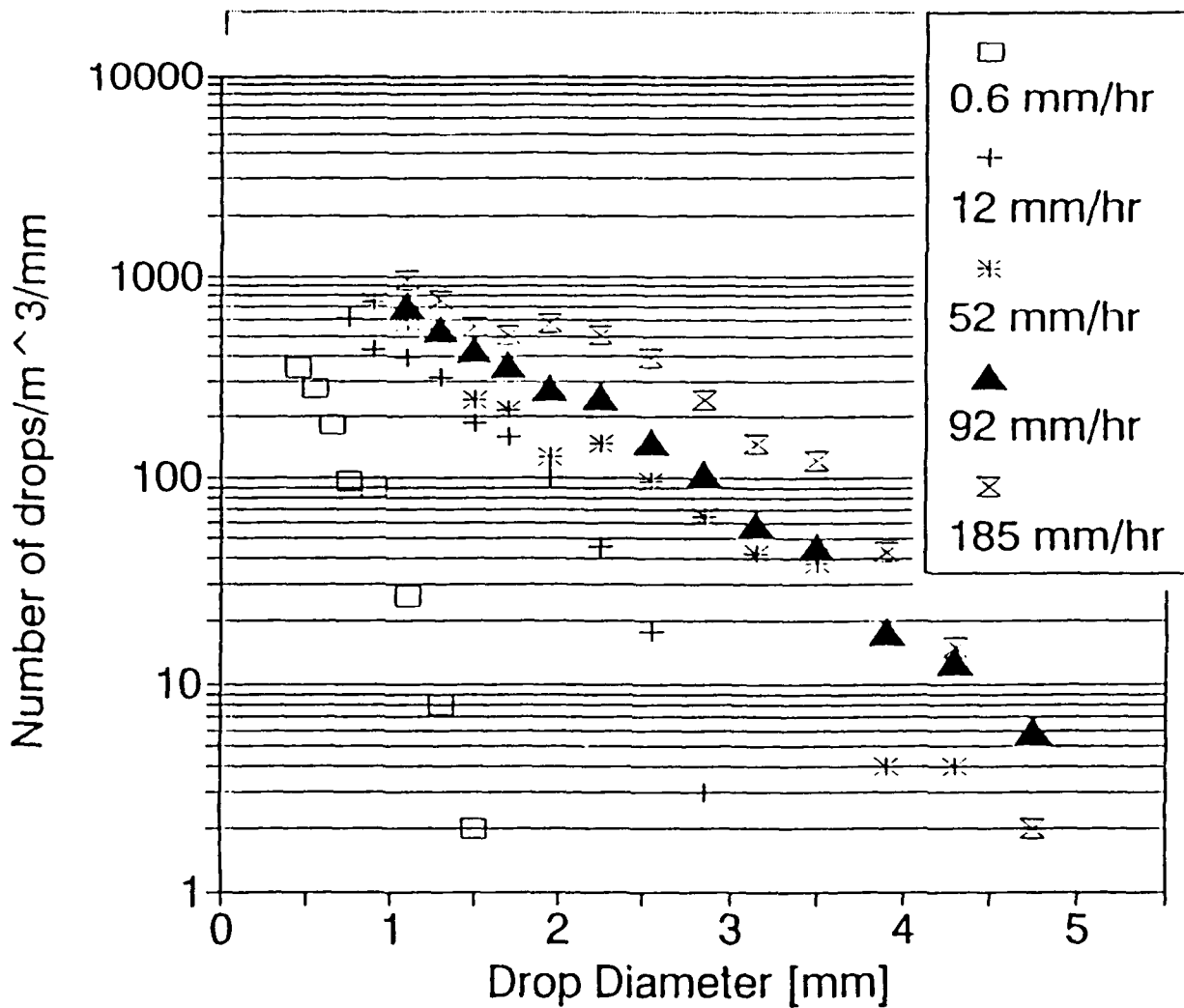


**Figure 6.** Typical raindrop size distributions showing number of drops per unit volume vs. drop diameter. Note that as rainfall rate increases, the number of large drops increases rapidly (courtesy of J.A. Nystuen).

the number of drops of all sizes, the rate of increase is most significant for larger drop sizes.

One might be concerned that when the wind speed is very high (> 10 m/s), the precipitation signal will be completely

obscured by noise from wind waves breaking. Nystuen and Farmer (1989) studied the acoustical signature of precipitation during frontal passages of Atlantic winter storms on the continental shelf of Nova Scotia. An important result from that experiment was the demonstration that even in strong wind conditions, an identifiable precipitation signal still can be detected. The correlation between the underwater sound and rainfall rate, wind speed, and wave height is obviously a complex one. Nystuen and Farmer (1989) did not attempt to quantify the correlation of rainfall rate and underwater sound. Their auxiliary rainfall measurement was of poor quantitative quality (weather radar only) and was not co-located with the hydrophone (separated by several kilometers).

This paper will attempt to quantify the correlation between rainfall rate and ambient sound using data from an ongoing experiment at the Ocean Test Platform (OTP) in the Gulf of Mexico. The experiment is designed to record acoustic data when the rainfall rate is heavy ( $>10$  mm/hr) so that large drops will be present. Auxiliary data is collected on the OTP and includes state-of-the-art optical rainfall rate measurements, wind speed and direction, wave spectra and overhead weather radar.

## II. EXPERIMENTAL SETUP AND DATA ACQUISITION

### A. EXPERIMENTAL SETUP

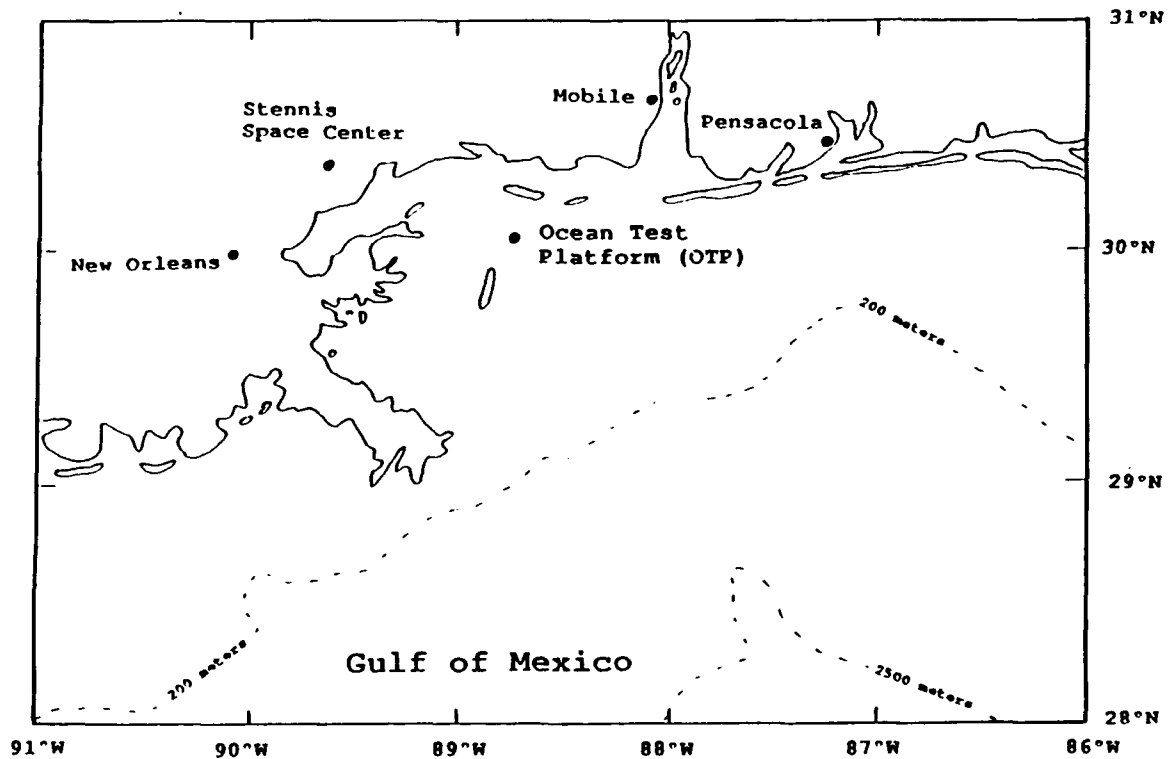
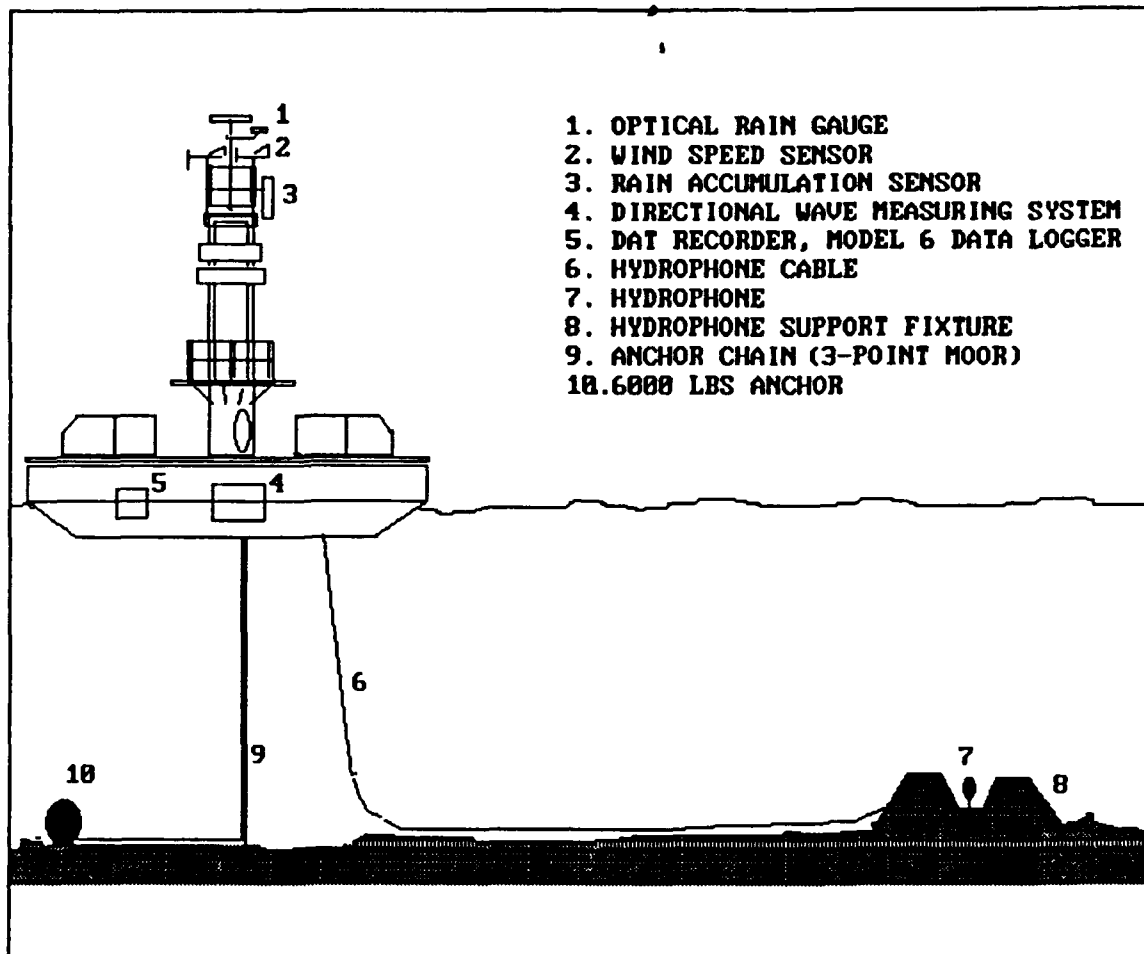


Figure 7. The location of Ocean Test Platform (OTP).

This study is part of the Ambient Noise Drifting Buoy Program being conducted by the Naval Postgraduate School (NPS) and the National Data Buoy Center (NDBC) to understand the sound generated by heavy precipitation under a variety of conditions. This experiment was conducted at NDBC's Ocean Test Platform (OTP) in the Gulf of Mexico about 40 kilometers off



1. OPTICAL RAIN GAUGE
2. WIND SPEED SENSOR
3. RAIN ACCUMULATION SENSOR
4. DIRECTIONAL WAVE MEASURING SYSTEM
5. DAT RECORDER, MODEL 6 DATA LOGGER
6. HYDROPHONE CABLE
7. HYDROPHONE
8. HYDROPHONE SUPPORT FIXTURE
9. ANCHOR CHAIN (3-POINT MOOR)
10. 6000 LBS ANCHOR

Figure 8. The Ocean Test Platform (OTP).

the coast of Mississippi (Figure 7). The OTP is a large platform (10 m in diameter) permanently moored in water 15 meters deep (Figures 8 and 9). A small custom data acquisition system consisting of a hydrophone, recorder, optical and accumulation rain gauges and anemometer were assembled and installed on OTP. At this site, regular measurements of ocean surface conditions including wave height and direction, wind speed and direction, air/sea temperature difference, and

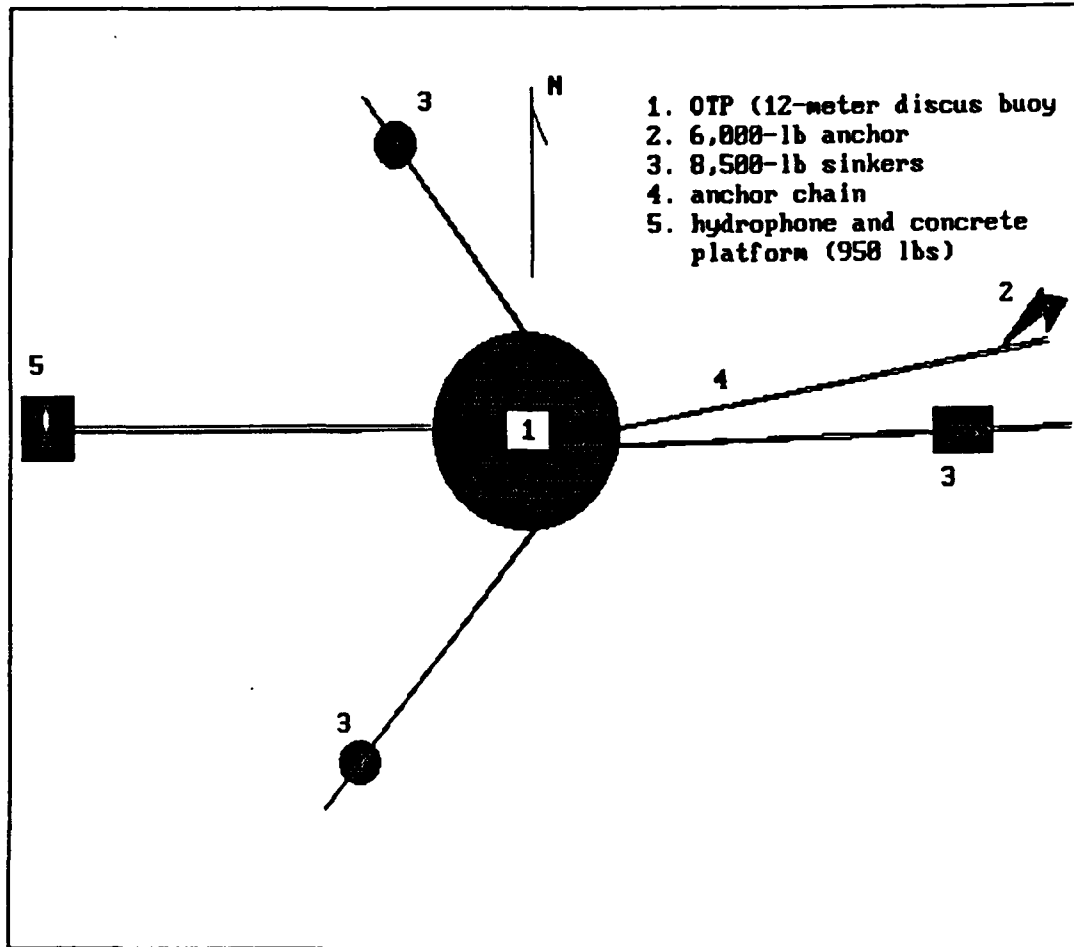


Figure 9. The OTP mooring design.

precipitation are automatically recorded and reported via GOES satellite communication link to NDBC. In addition, the OTP site is also in the coverage area of the weather radar at Slidell, LA.

## B. DATA ACQUISITION

### 1. ACOUSTICAL RECORDING

Digital recordings of ambient sound were collected by mounting a modified ITC Model 3001 hydrophone, with an

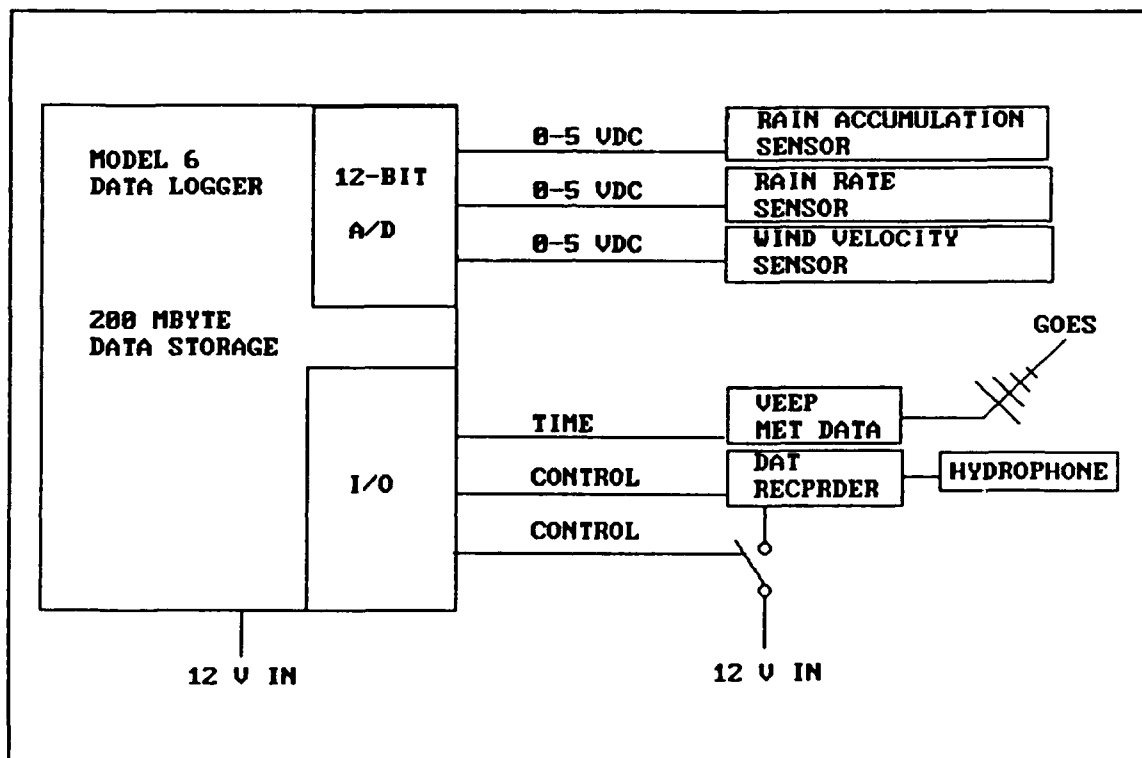


Figure 10. Control diagram of meteorology and acoustic data acquisition.

integral 23 dB amplifier in a cement block on the bottom (water depth 13 meters) approximately 70 meters from the OTP (to attempt to avoid noise generated by the OTP itself). The hydrophone has a narrow upward pointing beampattern to

attenuate any noise from the buoy (Figure 8). The acoustical data were transmitted to the OTP by cable and recorded digitally. A model TCD-D10 PRO Sony Digital Audio Tape (DAT) Recorder was used to record acoustical signals at a 44,100 Hz sampling rate. The date and time were tagged digitally on the tape and are available on the front panel of the recorder during playback to correlate the acoustic recording with data from the other sensors. An Onset Computer Model 6 data logger was used to monitor two rain gauges, an anemometer, and to control the RECORD function on the DAT recorder. The Model 6 Data logger has a 8-channel, 12-bit A/D converter, 14 digital I/O lines, and a 200 Mbyte hard disk drive. The optical rain gauge was continuously monitored. When the rainfall rate exceeded 10 mm/hr, the DAT recorder was turned on and the acoustical signals were recorded. Any combination of wind speed and rate of rainfall could have been used to trigger the recording of data. The rate 10 mm/hr was chosen so that data would be from heavy rain only. The data from the two rain gauges and the wind speed sensor were sampled at a 1 Hz rate and stored on the 200 Mbyte hard drive for the times that the DAT recorder was active (Figure 10). The data was then transferred to a 5.25 inch floppy disk. Along with the recorder tape, this disk was sent to NPS for data analysis.

## **2. ENVIRONMENTAL DATA**

### **a. OPTICAL RAIN GAUGE**

A Scientific Technology, Inc optical rain gauge Model ORG-705C was used to monitor the rainfall rate. This rain gauge has a 0-5 VDC output which was fed directly to data logger A/D channel with 1% accuracy over the range 10 to 100 mm/hr and 10% over the range .5 to 1000 mm/hr. The optical rain gauge was installed at the 10-meter level of the buoy and monitored continuously to determine when to begin a recording on the DAT recorder.

### **b. RAIN ACCUMULATION SENSOR**

A RM Young model 50202 rain accumulation sensor was used to monitor the total accumulated rainfall. This sensor output was fed directly to the data logger. This sensor was also installed at the 10-meter level.

### **c. WIND SPEED SENSOR**

A RM Young anemometer was used to record the wind speed and direction whenever the acoustical data is being recorded. This sensor has a 0-14 VDC output and this signal was buffered through a voltage divider and fed to the data logger. The sensor was also installed at the 10-meter level.

### **d. WAVE DATA**

The OTP buoy has two wave measuring systems which report wave data hourly through the GOES network. Wave spectral data,

significant wave height, and wave period data are available and are archived at the NDBC Computer Center.

**e. NATIONAL WEATHER SERVICE RADAR DATA**

Local weather radar plots were generated for the times when the acoustic recording system was active. These plots provide a reference for comparison with in-situ rainfall rate measurements and show the areal coverage of the storms.

**C. DATA PROCESSING**

During the first stage of the experiment (July 24 - August 30 1990), nine independent events of various rainfall rates were recorded, ranging from rain-free to very heavy rain (greater than 300 mm/hr). These digitally recorded sound signals along with environmental data recorded at the same time were sent to NPS for data analysis. By using a Sony Digital Pulse Code Modulator (PCM), these acoustic signals were sent to a HP computer where a Fast Fourier Transform (FFT) algorithm was used to obtain the sound spectrum. The raw data were converted to sound intensity by:

$$I=10*\log[A(\frac{count^2}{\Delta f}) * B(\frac{volt^2}{count^2}) * C(\frac{\mu Pa^2}{volt^2})] \quad (3)$$

Here I is sound spectral level in dB relative to  $1 \mu Pa^2/Hz$ , A is the output of the FFT algorithm, B is recorder frequency sensitivity (obtained from a white noise voltage generator),

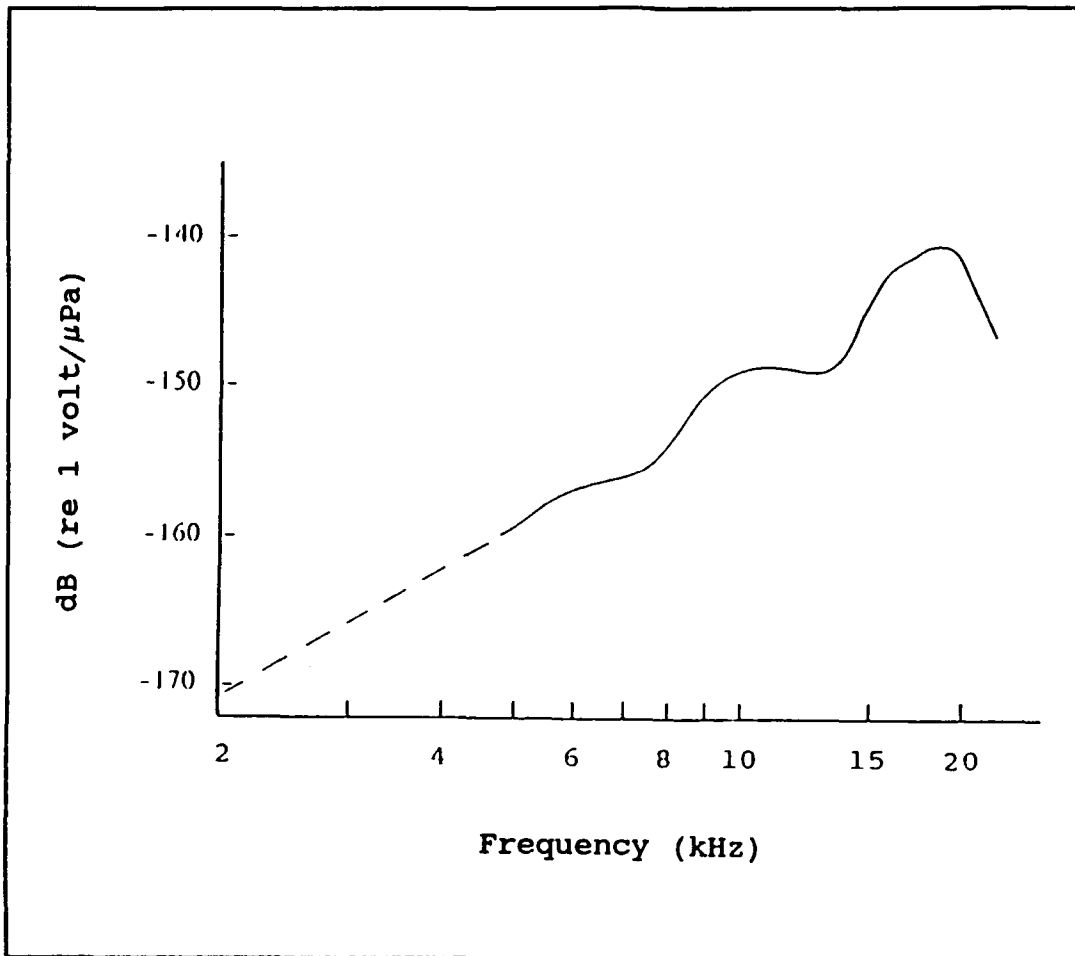


**Figure 11.** The free field sensitivity curve of the ITC Model 3001 hydrophone.

and C is the hydrophone sensitivity (from the manufacturer). The hydrophone sensitivity was reported from 5 to 22 kHz (Figure 11). The sensitivity curve was extrapolated to 2 kHz assuming a linear trend. It was later found that sound spectral levels at 2 kHz obtained by this method are about 15-20 dB higher than the results of other studies. Furthermore, the resulting spectra show consistent fine structure (2-3 dB) at local maxima in the hydrophone sensitivity curve (Figure

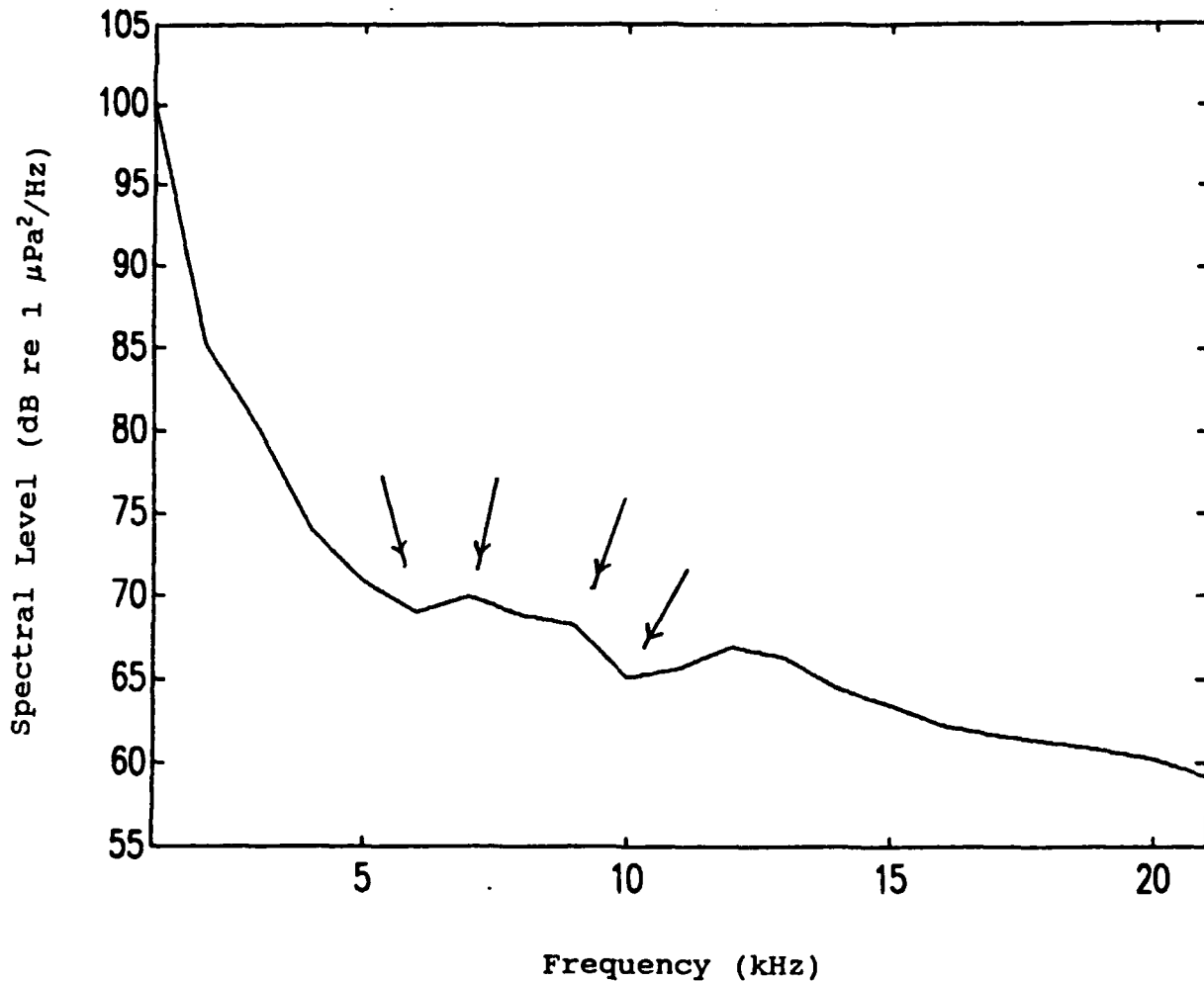


**Figure 12.** An example of the sound level spectrum from rainfall rate = 16 mm/hr and wind speed = 3.8 m/s. The fine structure indicated by arrows is always present from 6 to 10 kHz. This is believed to be due to an improper hydrophone sensitivity correction.

12). These findings demand that the hydrophone sensitivity calibration be rechecked particularly for the mounting used. However, the comparison of the correlation of the sound at any given frequency with rainfall rate will not be affected by an error in the hydrophone sensitivity. Absolute pressure levels will, of course, be in doubt.

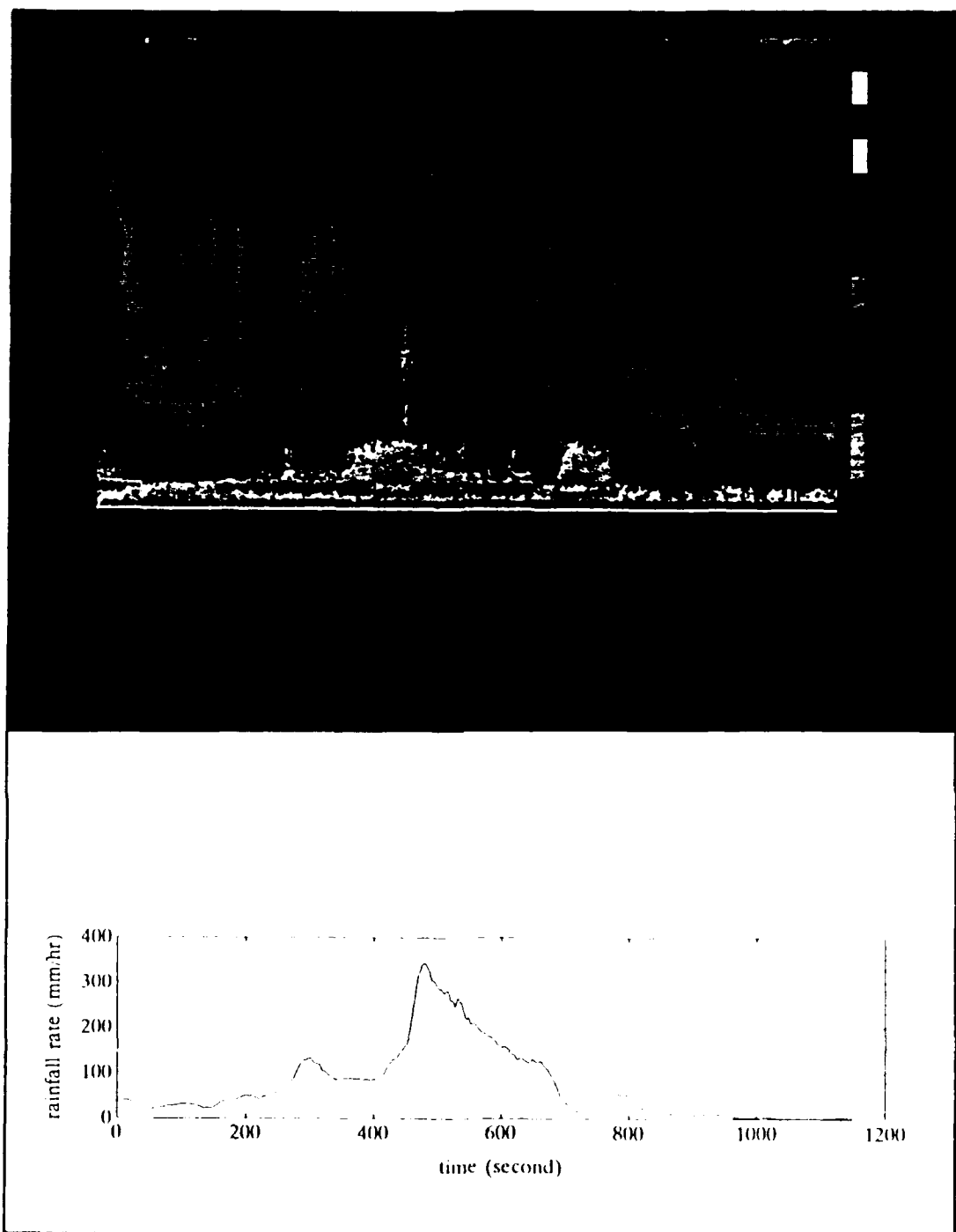
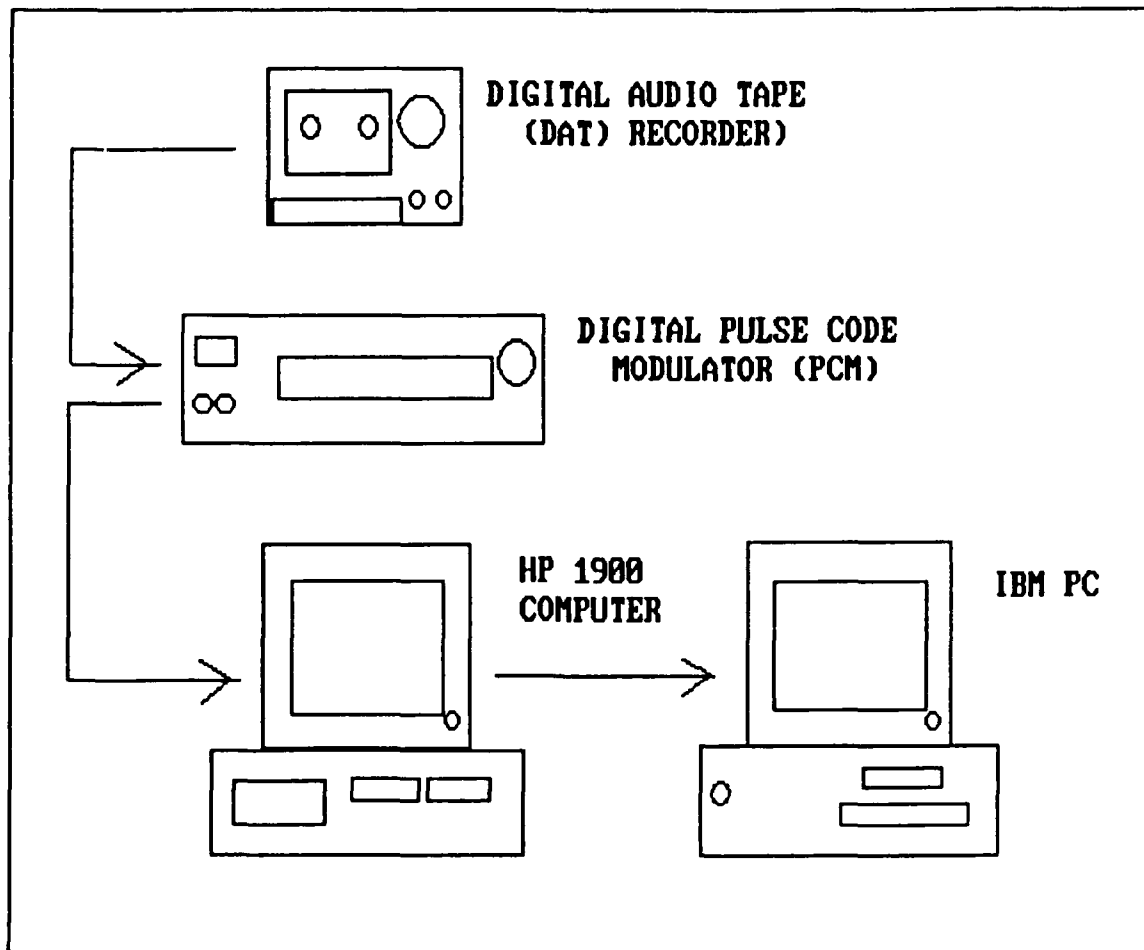


Figure 13. Upper: Sonogram of the underwater sound caused by rainfall. The different colors represent different spectral levels in dB rel.  $1 \mu\text{Pa}^2/\text{Hz}$ . Lower: Same time series of the rainfall rate measured by the rain gauge.



**Figure 14.** Block diagram of data processing.

The processing algorithm used to analyse the ambient sound data generated a color "waterfall" sonogram. In this display, the x-axis is the time series in seconds and y-axis is frequency from 0 to 22.5 kHz. Each color represents a different sound intensity level (from 40 to 110 dB rel. to  $1 \mu\text{Pa}^2/\text{Hz}$ ). The auxiliary data can be aligned for easy comparison (Figure 13). There were actually two modes of the processing program developed. One used running 512 points FFT

in real time to generate a time series with a time step of one second (to compare with the environmental data). In this mode 86% of the acoustical data is missed because of the processing time. The tape recorder runs continuously while the computer reads, then processes data, then reads more data, processes it, and so on. Approximately 12 spectra are processed in one second (14% of the data), giving 24 degrees of freedom. To increase the degrees of freedom, every 12 points in frequency domain were averaged, thus each sonogram consists of 21 frequencies, each frequency has a bandwidth of 1 kHz with 36 degrees of freedom. A time series of these 21 frequency bands were then written onto a floppy disk for further analysis on a IBM PC (Figure 14).

The other mode of the program defined a computer buffer into which a short time block of continuous data was written (e.g. 500 ms). This block of continuous data was analysed by extracting 64 data points (1.25 ms) at a time and running a 64 point FFT. Owing to the limitation of the sampling rate of the recorder and the size of the buffer, the degrees of freedom in this mode is lower (just 2) when compared with the first mode. However, in this mode, the algorithm provides a chance to magnify, in time, the acoustical data and detect individual sound sources (bubbles). Snyder (1990) reports that individual large raindrops generate underwater sound at initial broadband impact followed 30-50 ms later by a single very energetic large "dominant" bubble (2-10 kHz) approximately 50% of the

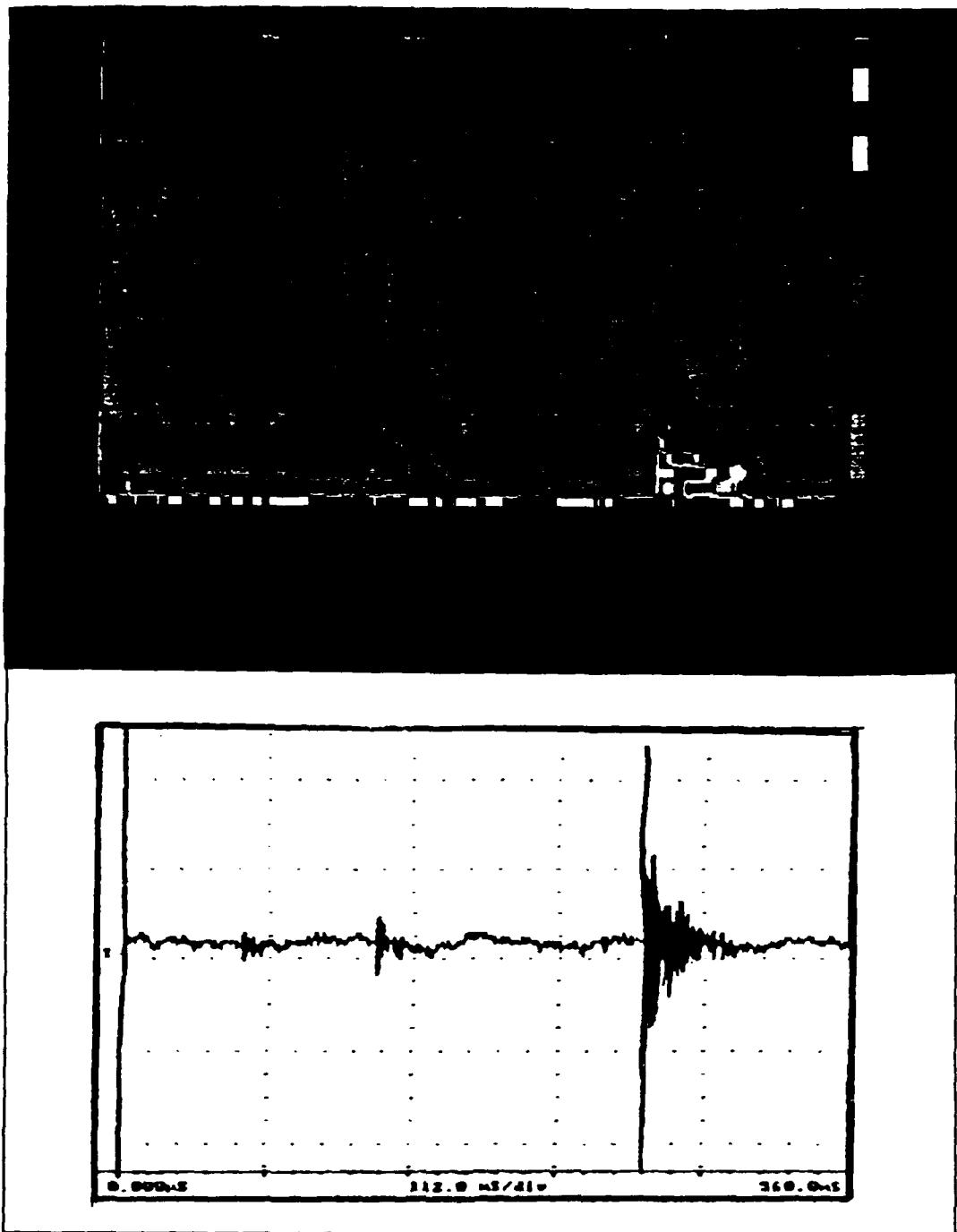
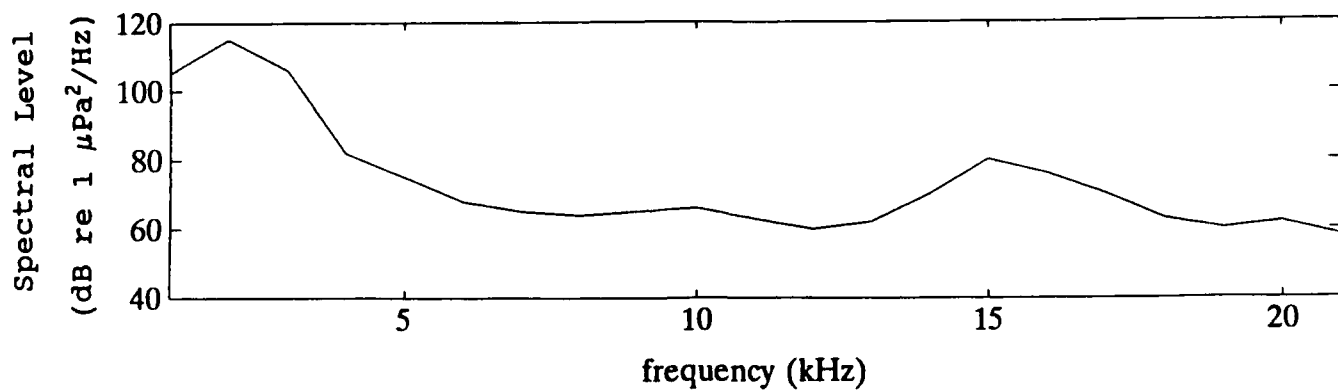


Figure 15. Sonogram of three splashes by large raindrops (upper) compared with the same time series generated by oscilloscope (lower). This event was recorded in a canal at the Stennis Space Center when large individual drops well separated in time were falling.

time plus several smaller less energetic "secondary" bubbles. Figure 15 shows a 580 ms record of the sound time series showing three individual splashes by large raindrops. The very energetic bubbles which resonate at narrow and well-defined frequencies are clearly detected (Equation 1). The event at  $t=410$  ms shows the dominant bubble at 2 kHz, with secondary bubble at 15 kHz (Figure 16). Roughly 30 ms prior to this event there is a weak broadband signal, possibly the impact. The impact sound is certainly much weaker than the subsequently entrained bubbles. The damping time (to  $e^{-1}$  amplitude) for a bubble is:

$$t_e = \frac{1}{\pi f \delta} \quad (\text{Medwin and Clay, 1977})$$

Where  $f$  is the bubble frequency,  $\delta$  is the resonance damping constant (e.g. 0.06 for 16 kHz bubble). The resulting -8 dB change in intensity level per damping time at 2 kHz and 16 kHz are consistent with those shown on Figure 15. At  $t=200$  ms, a less energetic dominant bubble is detected at 2 kHz with secondary bubbles at 7 and 20 kHz. The damping rate for these bubbles is also consistent with theory. The event at  $t=110$  ms is not clearly seen. However, it still shows a probable bubble resonant at 6 kHz. Compared with the figure generated by the oscilloscope time series (see Figure 15), the spectral description by the sonogram yields a clearer identification of these individual bubbles.



**Figure 16.** Sound spectrum caused by a drop splash (Figure 15 at  $t=410$  second). The peak at 2 kHz is caused by a dominant bubble. Also observed is a less energetic peak at 15 kHz which indicates a secondary bubble.

### III. DATA ANALYSIS

#### A. PREDEPLOYMENT OBSERVATIONS

Prior to deployment at the OTP, the hydrophone system was tested in a canal at the Stennis Space Center on July 10. During this test a convective storm passed over the area. Acoustical data of a light rain was collected. Auxiliary data is qualitative in nature, however wind speeds were very light. The rain became heavier during the second half of this event, with "gurgling" associated with larger drops detected.

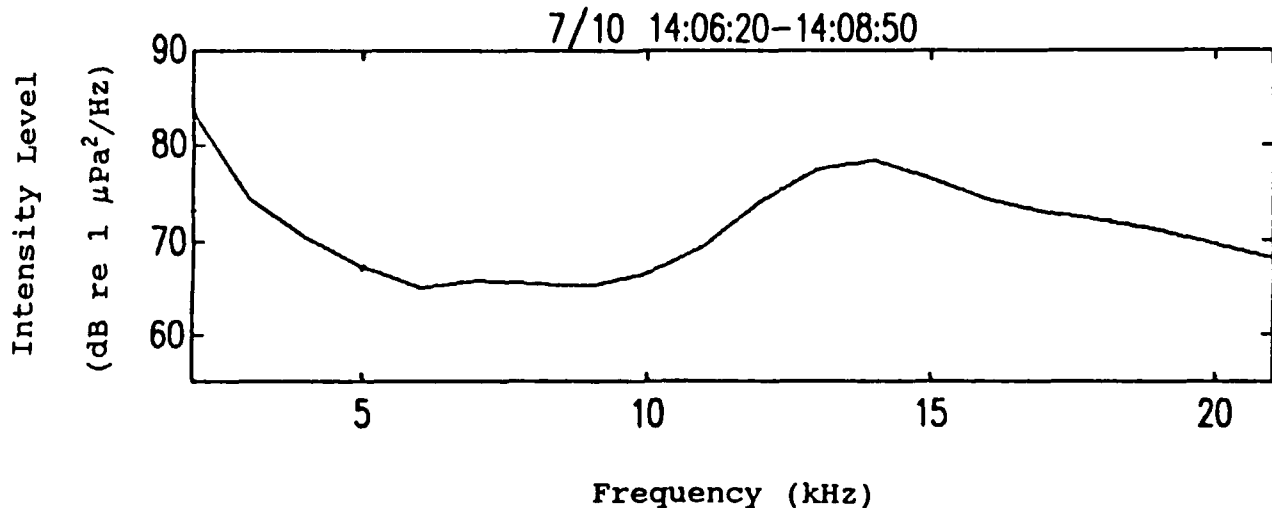


**Figure 17.** Spectrum of sound under light rain, light wind conditions which was obtained by averaging over 150 seconds. A peak at 14 kHz is observed.

During first half of this event, a peak of 85 dB at 14 kHz is observed which shows a sharp cutoff on the low-frequency

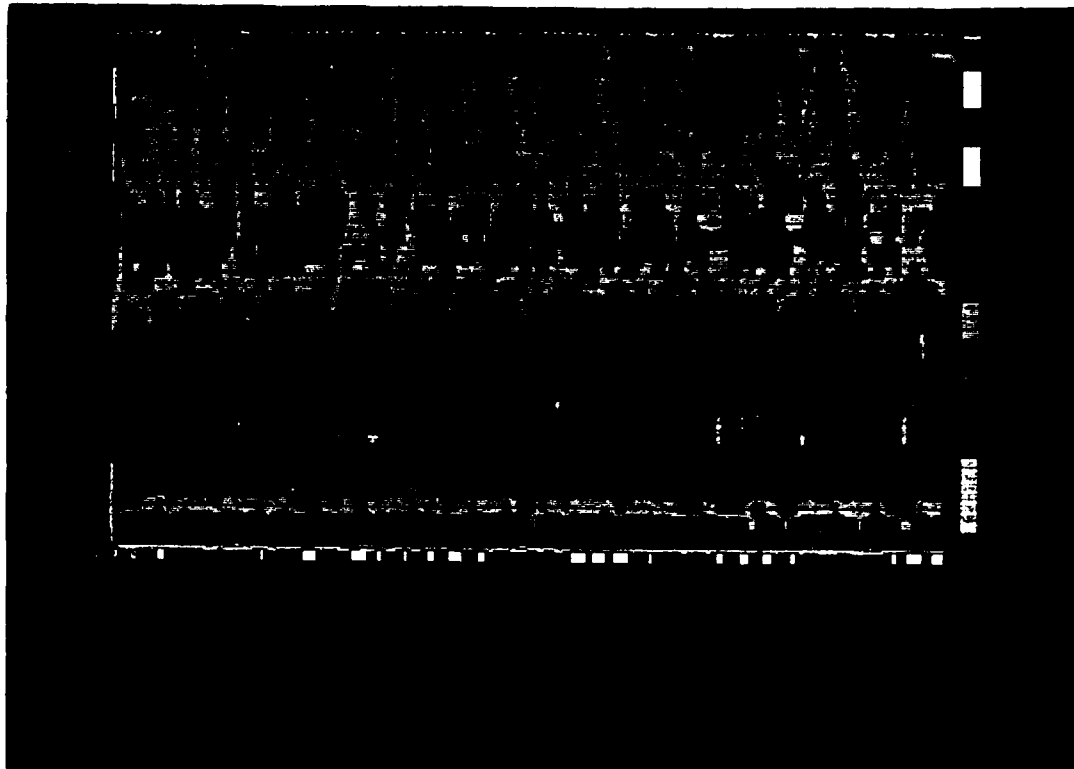


**Figure 18.** A 580 ms sonogram of a light rain under light wind conditions which shows numerous acoustical events (individual bubbles) in the frequency range 13-15 kHz.

side and a gradual fall-off on the high-frequency side (Figure 17). This structure agrees with the sound spectra in light rain and light wind conditions observed by Nystuen and Farmer (1987), Scrimger et al. (1989). It is attributable to bubbles created by raindrops of diameter  $\approx 1$  mm striking the surface at near normal incidence (Nystuen, 1990). Figure 18 shows a 580 ms record during this period. Numerous acoustical events are detected in the frequency range 14-18 kHz. A histogram of the bubble sound generated during this half second interval is compared to the frequency distribution of bubbles generated by

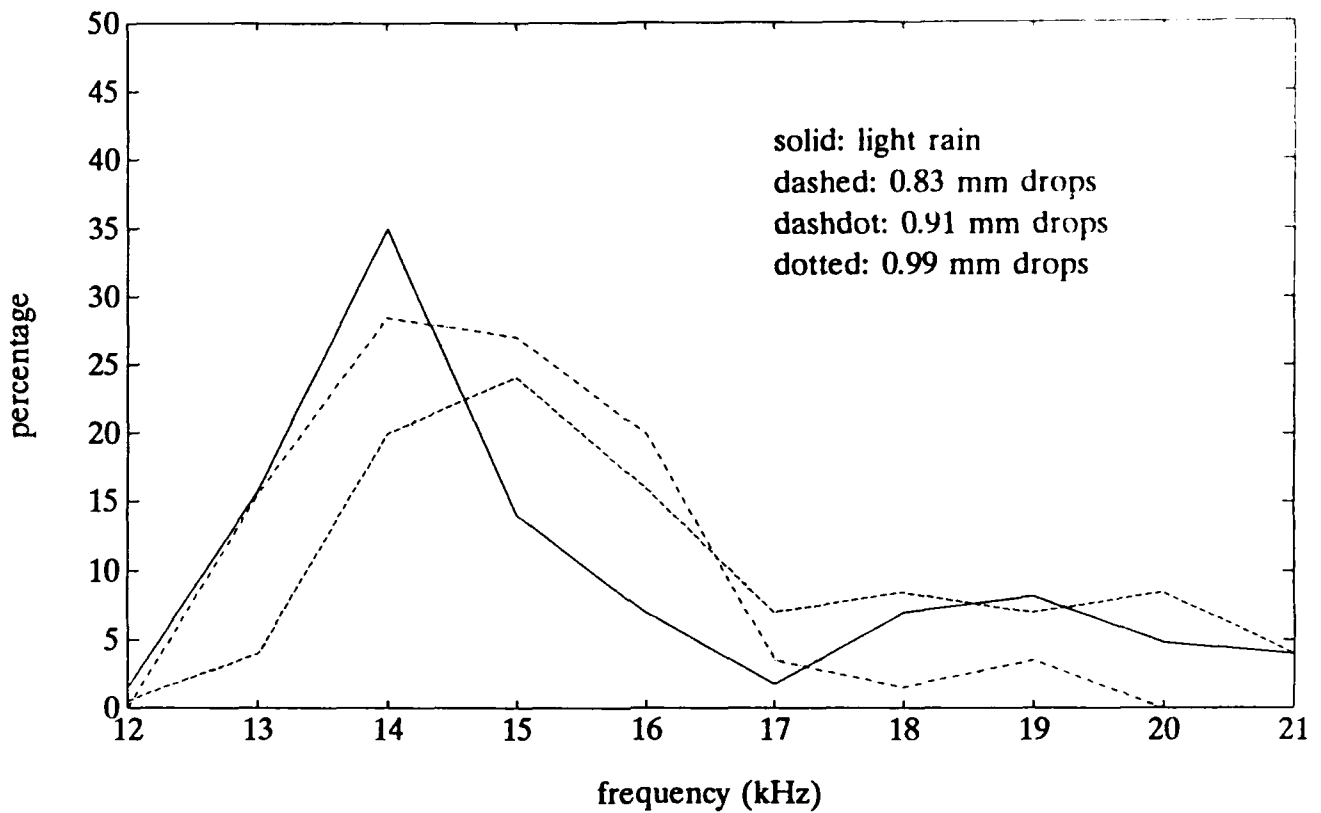


**Figure 19.** Histogram of the resonance frequencies of bubbles generated in light rain compared with the laboratory results of Medwin et al. (1990), which shows very similar shape with a peak at 14 or 15 kHz.

individual 0.8-1.0 mm drops impacting at normal incidence from a laboratory study (Medwin et al. 1989) (Figure 19). The resonance frequencies of bubbles from real rain have a very similar shape to that from the laboratory result. This result

strongly supports the conclusion that the 14 kHz peak observed during light rain is due to a limited range of small drop sizes (0.8-1.0 mm diameter) which are almost always present in natural rain.

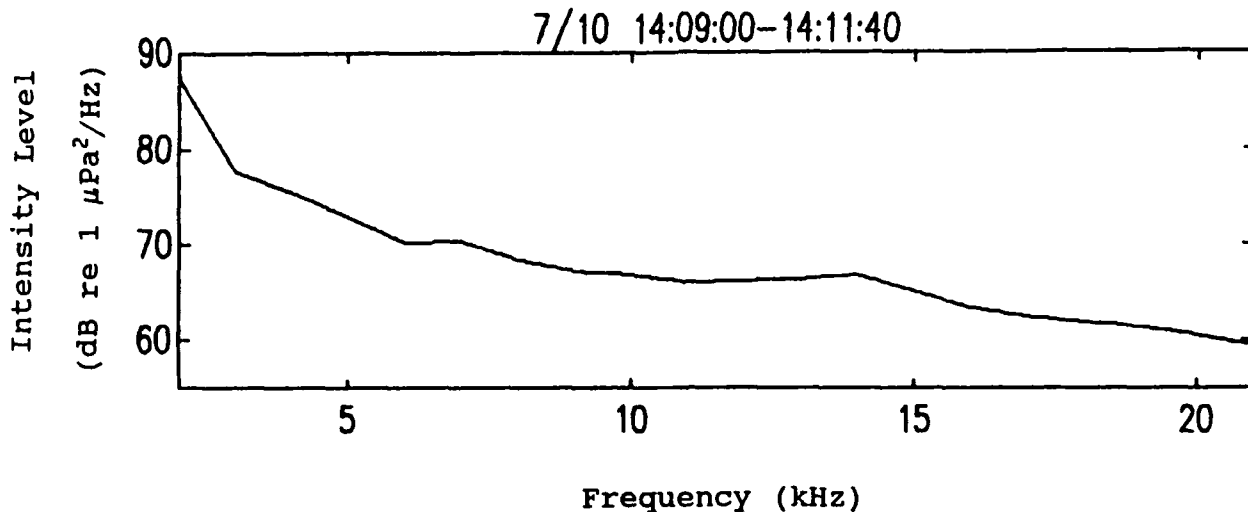


**Figure 20.** Spectral level of the underwater sound caused by a light rain with large drops falling onto the canal. The peak at 14 kHz present shown in figure 16 has disappeared.

This light rain was followed by a sudden change in the character of the rain. Gurglings associated with larger bubbles from larger raindrops are detected in the audio signal in this event. The peak at 14 kHz disappears and higher levels at low frequencies are detected (Figure 20). Figure 21 shows a 290 ms sonogram of this period. In this time series, 0.8-1.0 mm drops are probably still present (Figure 6 shows heavier rain usually increases drop concentrations at all drop sizes), yet the small bubbles (14-18 kHz) noted previously are now

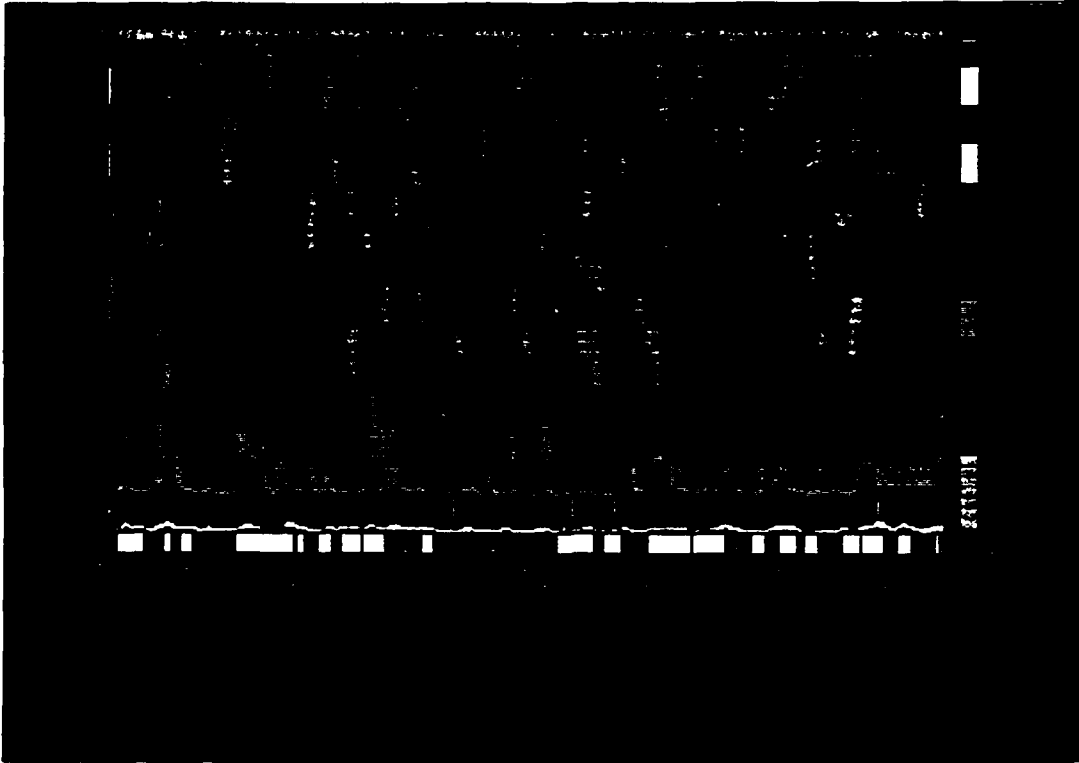


**Figure 21.** Sonogram (290 ms) of underwater sound when there are larger drops in light rain. Bubbles are now observed distributed throughout the spectrum.

absent. Apparently ripples from larger drop splashes create sufficient surface roughness to disrupt the bubble entrapment mechanism for 0.8-1.0 mm drops.

This event is shown more clearly in Figure 22, a 400 second sonogram showing the change in the character of the spectrum at the onset of the heavier rain. By taking the difference of the spectra before and after the change in the rain, the sound level difference shown in figure 23 indicating a decrease in acoustic levels from 10-22 kHz (the peak is suppressed) and increased sound levels at low frequencies

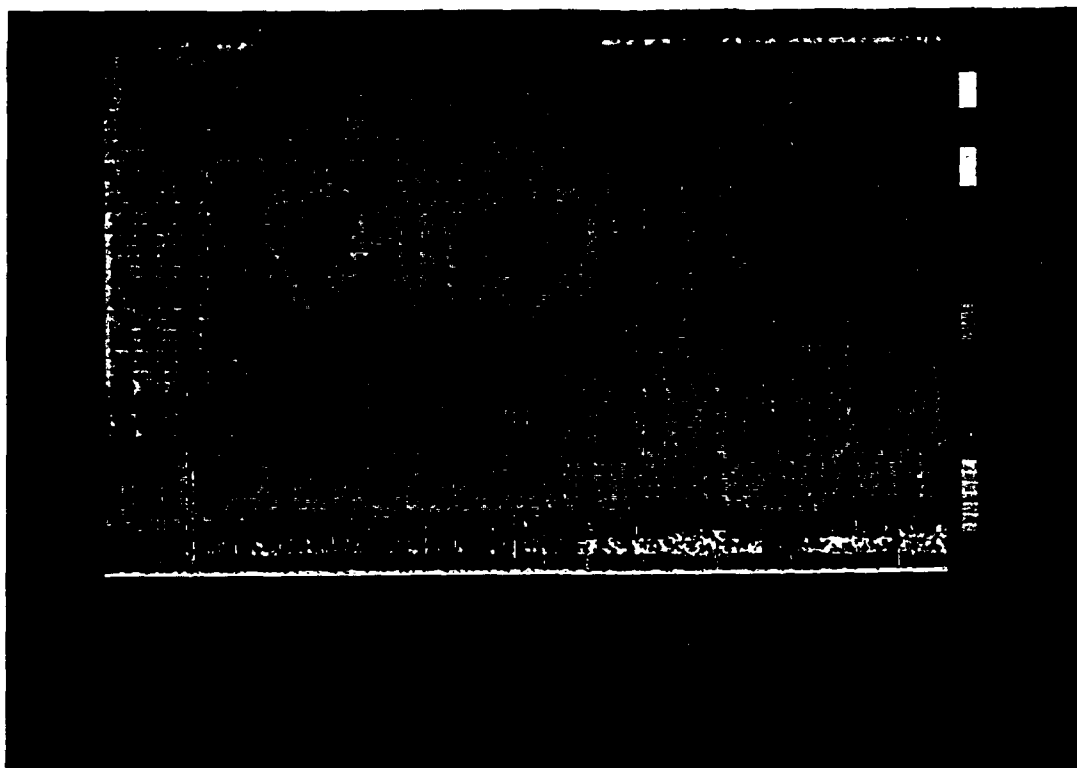


**Figure 22.** Sonogram (400 seconds) from the canal. The peak at 14 kHz disappears when gurgling sounds are heard (after 230 seconds). A tremendous increase in low frequency sound then occurs implying that larger raindrops are present in the rain.

(below 10 kHz), presumably due to larger bubbles generated by large raindrops.

#### **B. UNDERWATER SOUND SPECTRUM WITH NO RAIN**

The first data recorded at the OTP were triggered manually on July 24 during a period free of precipitation. The average wind speed was 3.2 m/s with wind direction 269° N. Since there was no rain, a "pure" wind spectrum was expected. Figure 24 shows the spectrum level time series at 5 kHz and 21 kHz. The

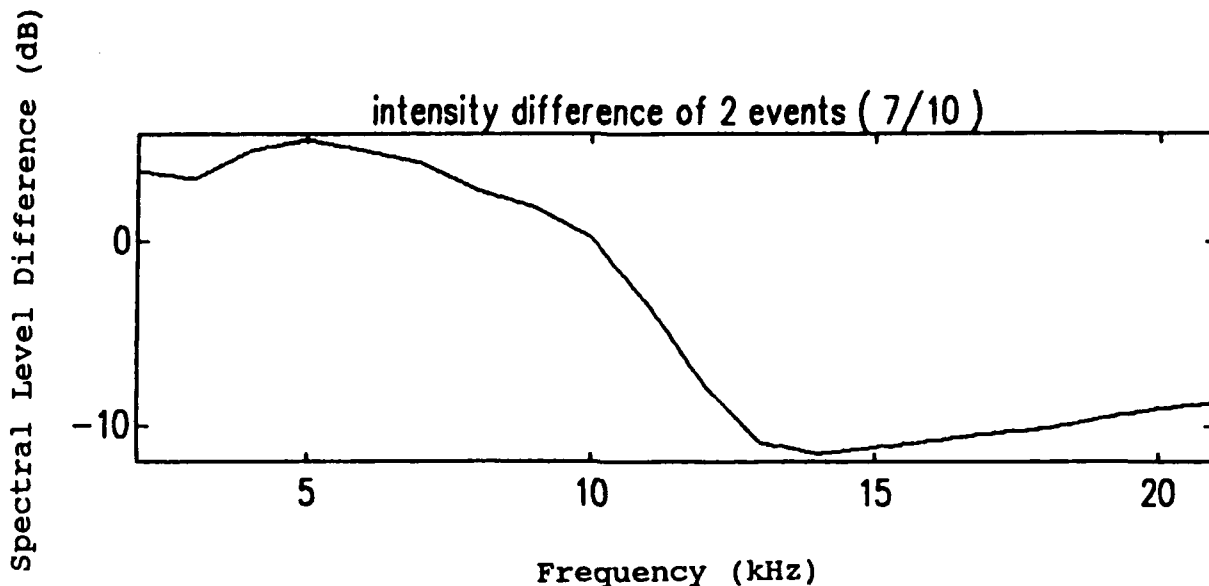


**Figure 23.** The spectral level difference of spectra recorded before and after the onset of larger drops in the rain.

levels at 5 kHz (44 dB) and 21 kHz (30 dB) agree with the expected levels (Figure 1).

**C. SOUND SPECTRA RECORDED UNDER CONDITIONS OF CONSTANT RAINFALL RATE WITH DIFFERENT WIND SPEEDS**

In a condition of light wind and light rain, the major effect of wind is to shift the spectral peak to a higher frequency and depress the spectral levels (Nystuen and Farmer, 1987). For higher rainfall rates, the spectrum has totally different characteristics than in light wind and light rain conditions. Figure 25 shows the spectrum caused by 8 mm/hr rainfall with two different wind speeds. Note that the

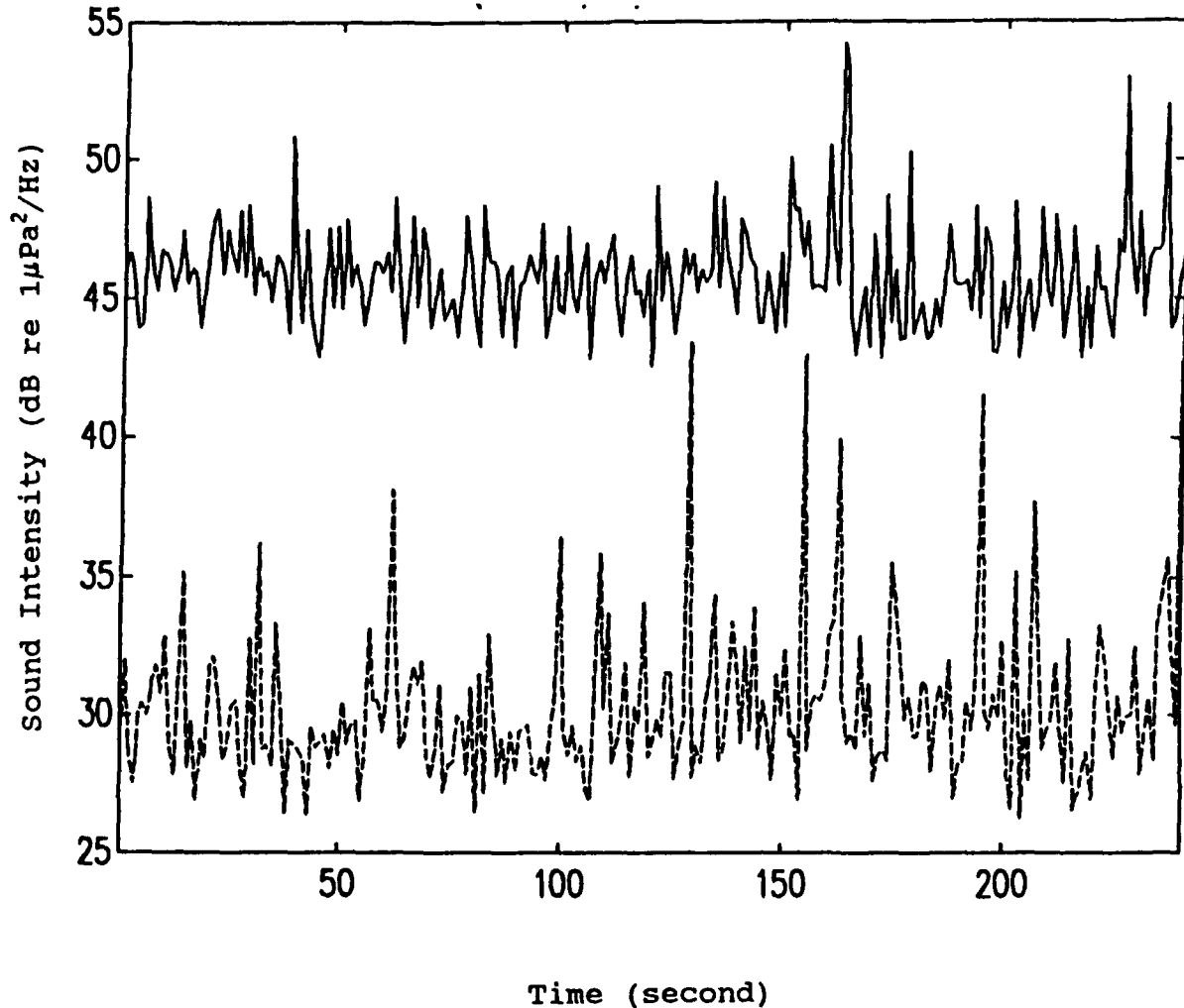


**Figure 24.** A 240 second time series of the spectral level at 5 kHz (solid) and 21 kHz (dashed) during constant 3.2 m/s wind with no precipitation measured on July 24.

spectral peak is not present. As the wind speed changes from 3.4 m/s to 5.6 m/s, the spectral level at frequencies above 10 kHz decreases. This may imply an additional suppression of sound generated by small drops as in the light rain situation.

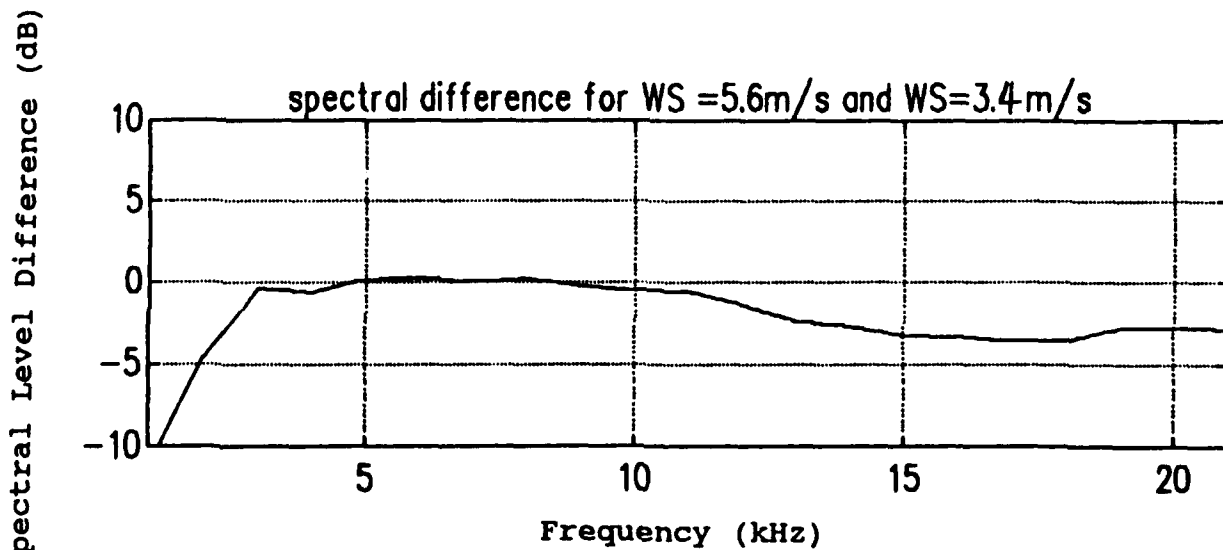
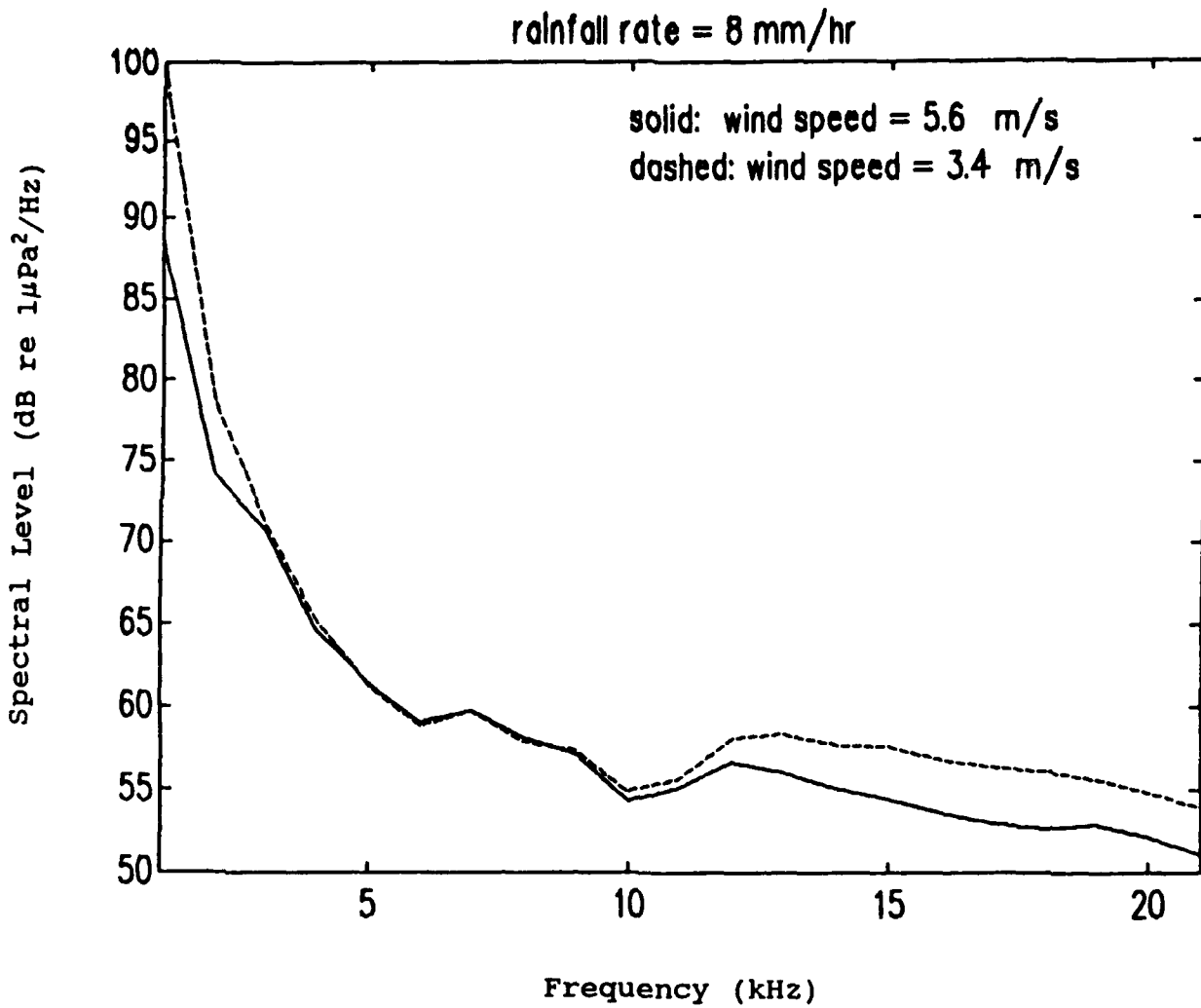


**Figure 25.** Upper: The underwater sound spectra during 8 mm/hr rainfall rate when wind speeds are 3.4 and 5.6 m/s. Lower: The spectral level difference of the two events ( $\text{SPL}_{\text{WS}=5.6} - \text{SPL}_{\text{WS}=3.4}$ )

There is no change from 3 to 9 kHz, the region where large drops have their dominant bubbles. The 5-12 dB difference below 2 kHz is partly due to a passing ship.

In Figure 26, the rainfall rate is 15 mm/hr. As the wind increases from 5.7 to 14.2 m/s, spectral levels increase below 12 kHz but decrease as a function of frequency above 12 kHz (to -11 dB at 21 kHz). This observation suggests attenuation due to ambient bubble clouds consisting of bubbles created by breaking waves at high wind speeds (Farmer and Lemon, 1984). Since the wind speed is very high (14.2 m/s), breaking waves are undoubtedly present. Ambient bubble clouds from the breaking waves are stirred down into the water and attenuate subsequent surface-generated sound attempting to pass through the bubble cloud. Little bubbles are stirred down most readily and so this effect is greatest at higher frequencies where these bubbles are resonant.

#### **D. SOUND SPECTRA RECORDED UNDER CONDITIONS OF CONSTANT WIND SPEED WITH DIFFERENT RAINFALL RATES**

Three examples of sound spectra caused by different rainfall rates are examined here. For a constant wind speed, Scrimger et al. (1989) suggest that the noise spectral levels will increase by +4 dB for each doubling of rainfall rate. Figure 27 shows a case with wind speed 5.5 m/s under two different rainfall rates recorded on August 23 two minutes

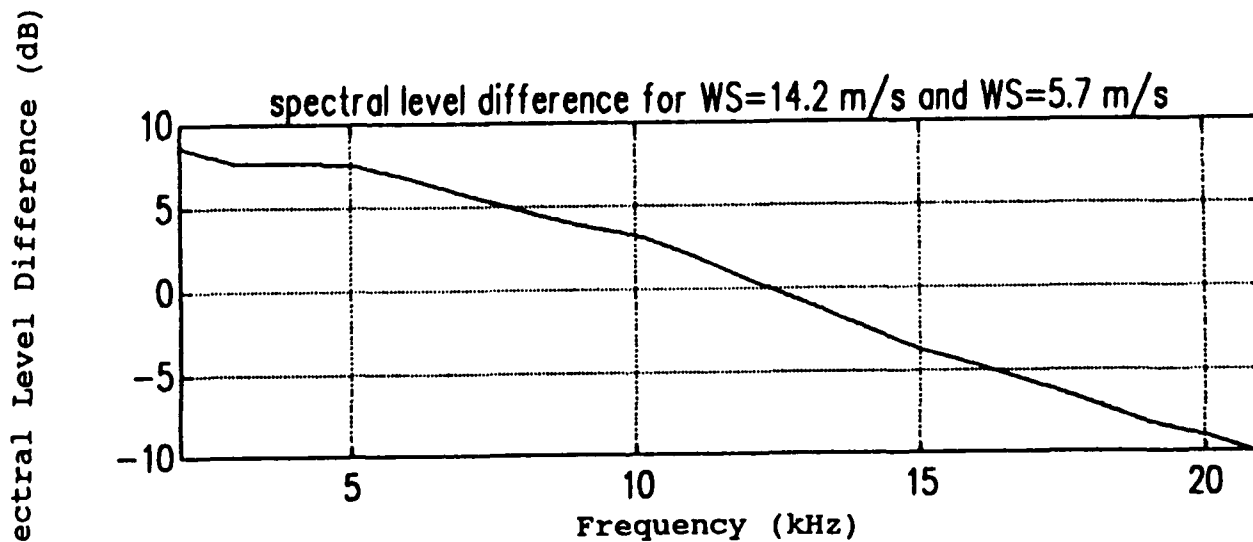
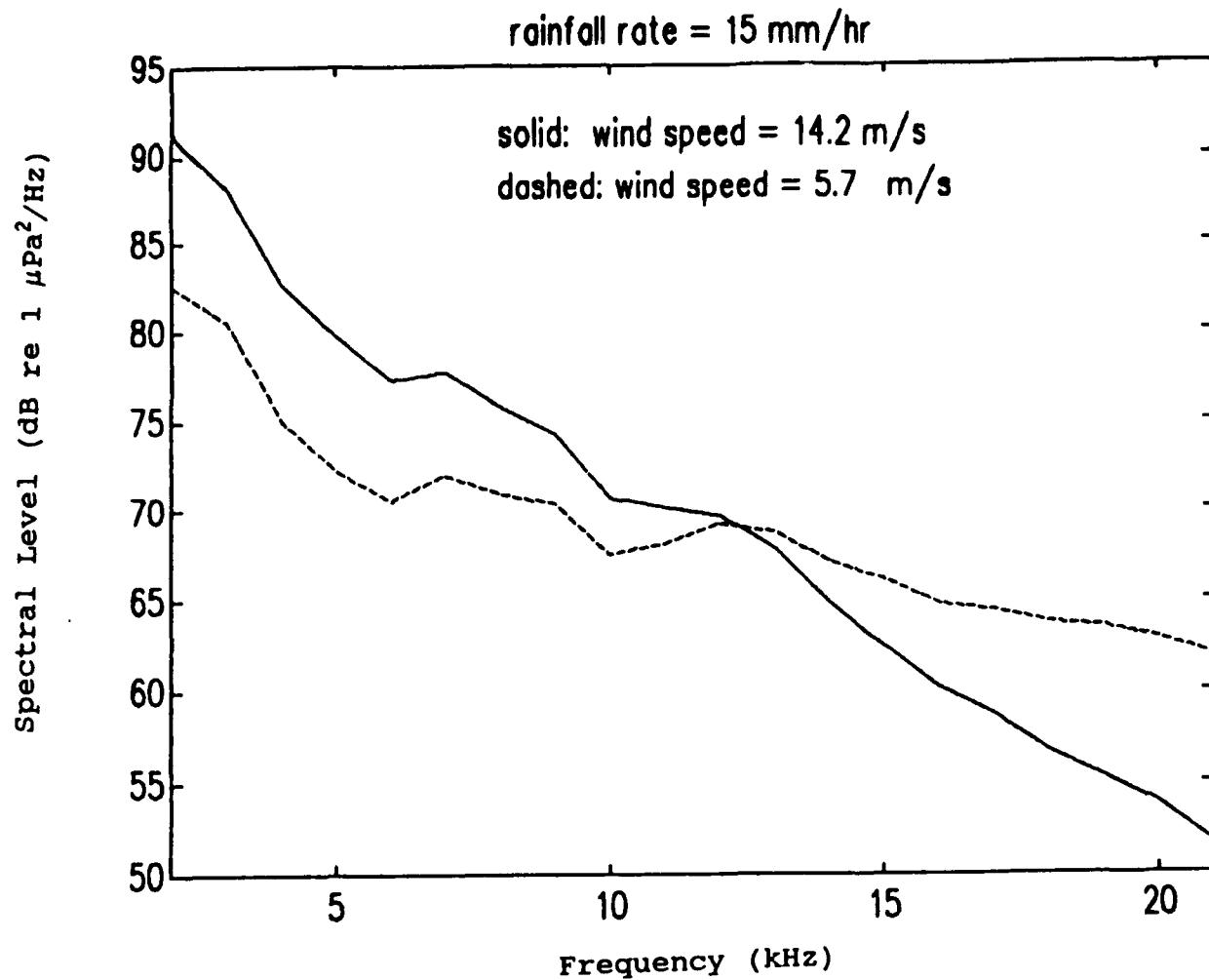


**Figure 26.** Upper: The underwater sound spectrum during 15 mm/hr rainfall rate when wind speeds are 14.2 m/s and 5.7 m/s. Lower: The spectral level difference of the two events ( $SPL_{WS=14.2} - SPL_{WS=5.7}$ ).

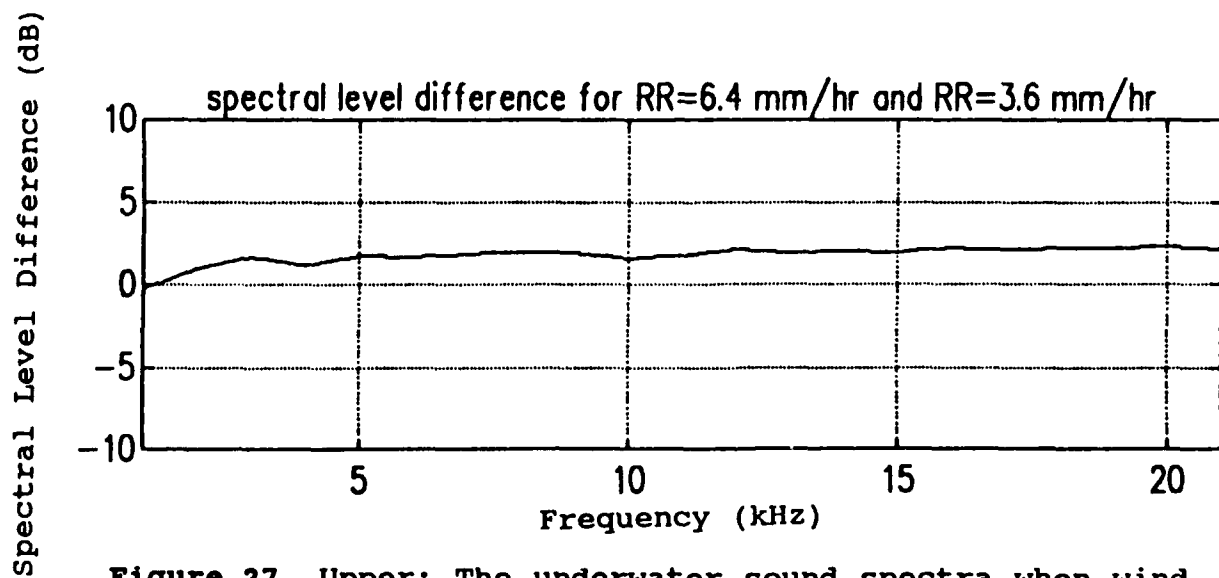
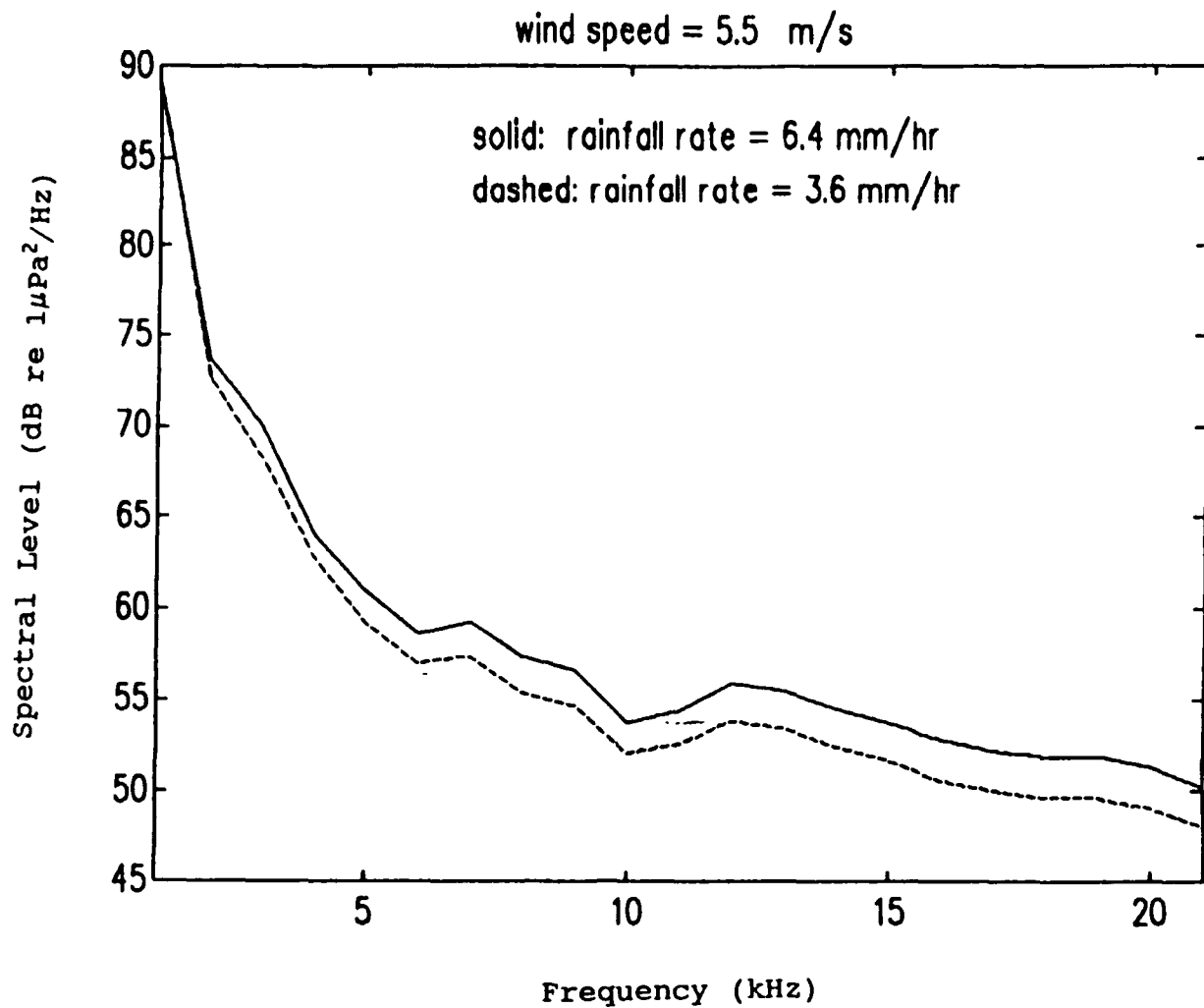


**Figure 27.** Upper: The underwater sound spectra when wind speed equals 5.5 m/s with rainfall rate 6.4 mm/hr and 3.6 mm/hr. Lower: Spectral level difference for the two events ( $SPL_{RR=6.4} - SPL_{RR=3.6}$ )

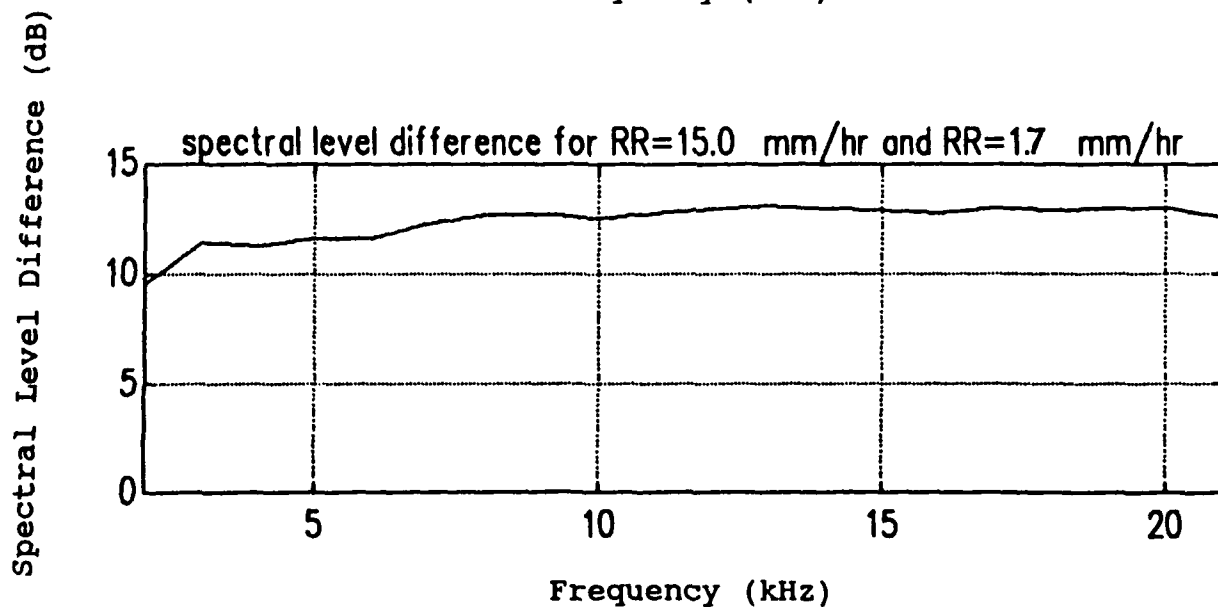
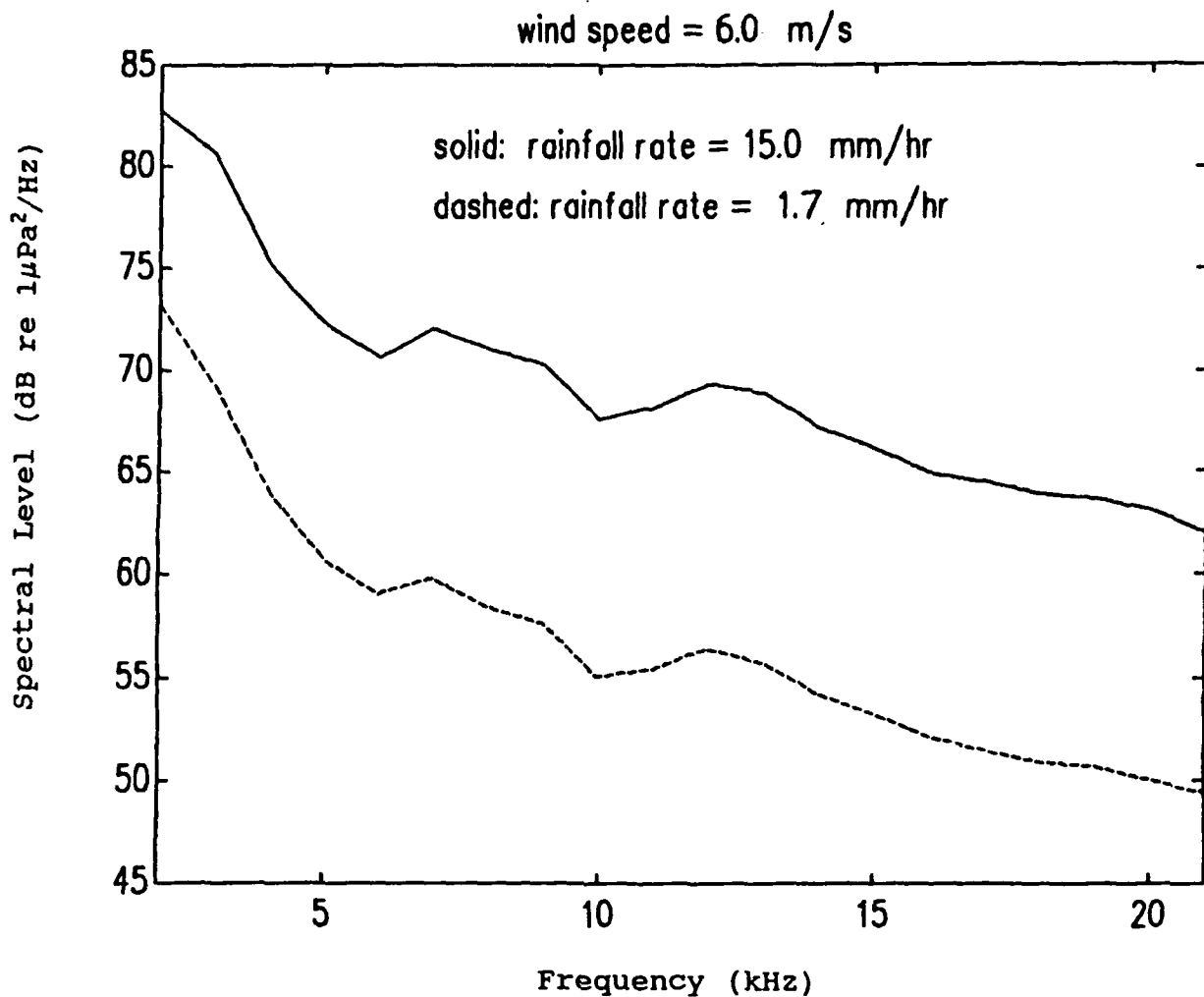
apart. All intensities increase as rainfall rate increases from 3.6 mm/hr to 6.4 mm/hr. There is a 2.5 dB intensity increase as rainfall rate increases by 70% which agrees well with that suggested by Scrimger et al.

Figure 28 shows the spectral levels for a case with wind speed 6.0 m/s. The higher rainfall rate (15.0 mm/hr) shows an increase of 12-13 dB when compared with the lower rainfall rate (1.7 mm/hr). This also agrees well with the result from Scrimger et al. The spectral levels at low frequencies (1-6 kHz) increase slightly less than those at higher frequencies (>7 kHz). It is not certain whether this was caused by a different drop size distribution in the rain or if a more complicated interaction of rain, wind and surface conditions had occurred. It appears to be true that the spectral level will increase as the rainfall rate increases.

In Figure 29 the rainfall rate has increased by 20% (from 5.8 mm/hr to 7.0 mm/hr). The sound intensity increases at low frequency (from 3 to 9 kHz), but there is no intensity difference from 12-21 kHz (opposite the previous example)! The most likely explanation for this situation is a sudden change in the drop size distribution of the rain. Unfortunately, the auxiliary data can not verify this possibility.

#### **E. VERY HIGH RAINFALL RATES**

A new finding in this study is that the same sound spectrum as observed during high wind speed conditions is



**Figure 28.** Upper: The underwater sound spectra when wind speed equals 6.0 m/s with rainfall rate 15.0 and 1.7 mm/hr. Lower: The spectral level difference of the two events ( $SPL_{RR=15} - SPL_{RR=1.7}$ ).

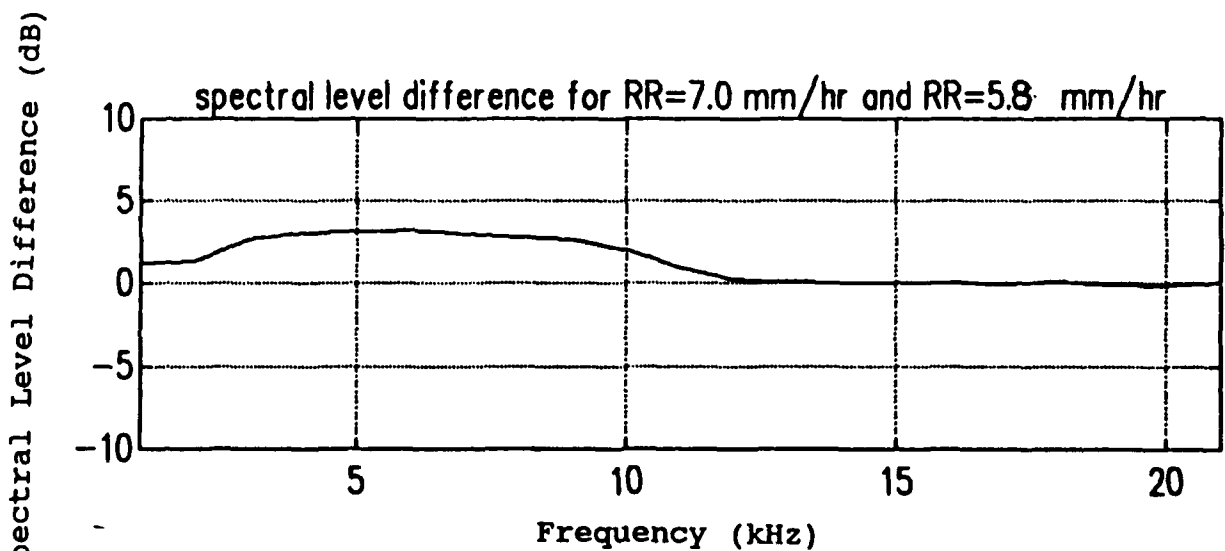
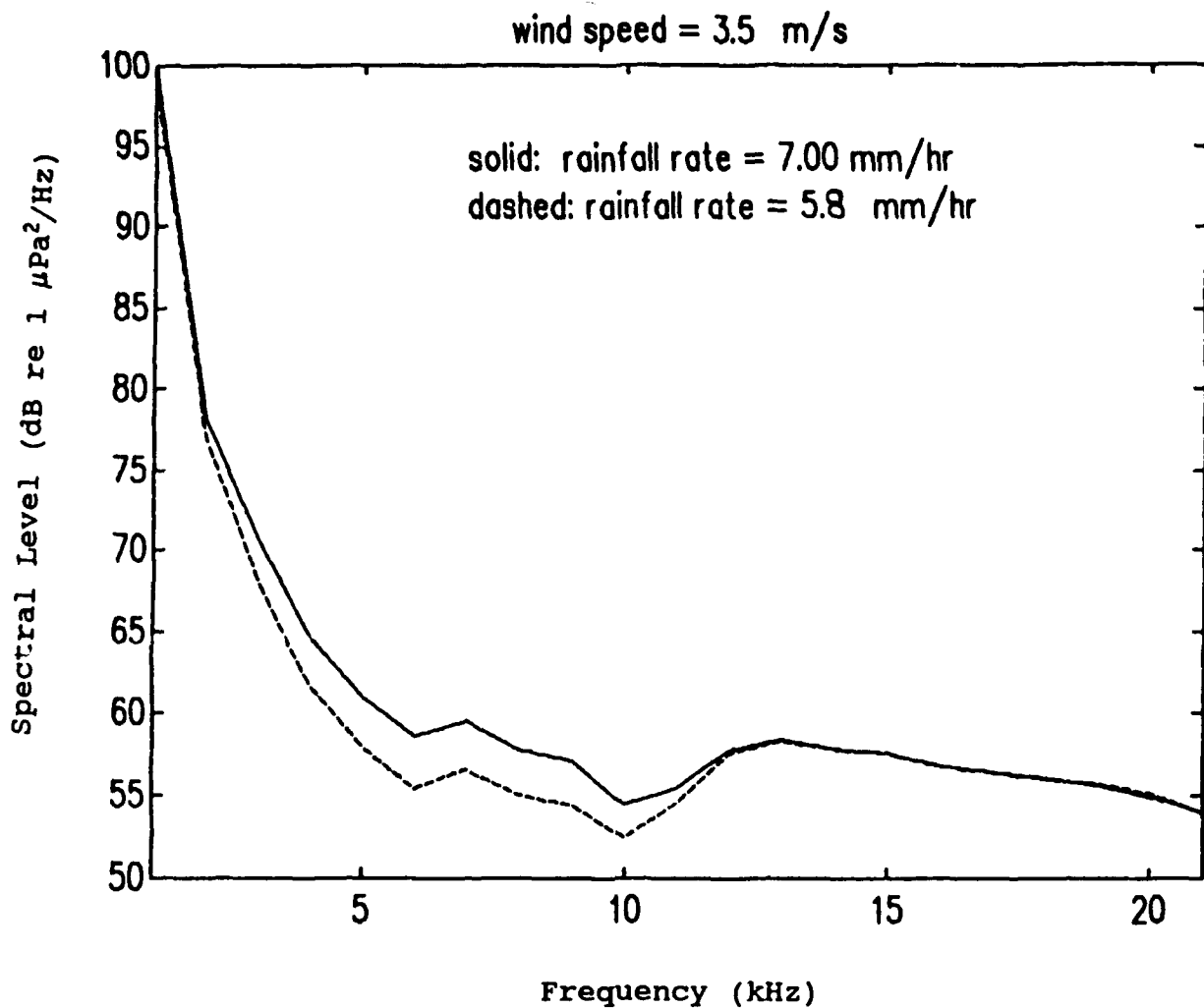


**Figure 29.** Upper: The underwater sound spectra when wind speed equals 3.5 m/s with rainfall rate 7.0 mm/hr and 5.8 mm/hr. Lower: The spectral level difference of the two events ( $SPL_{RR=7.0} - SPL_{RR=5.8}$ ).

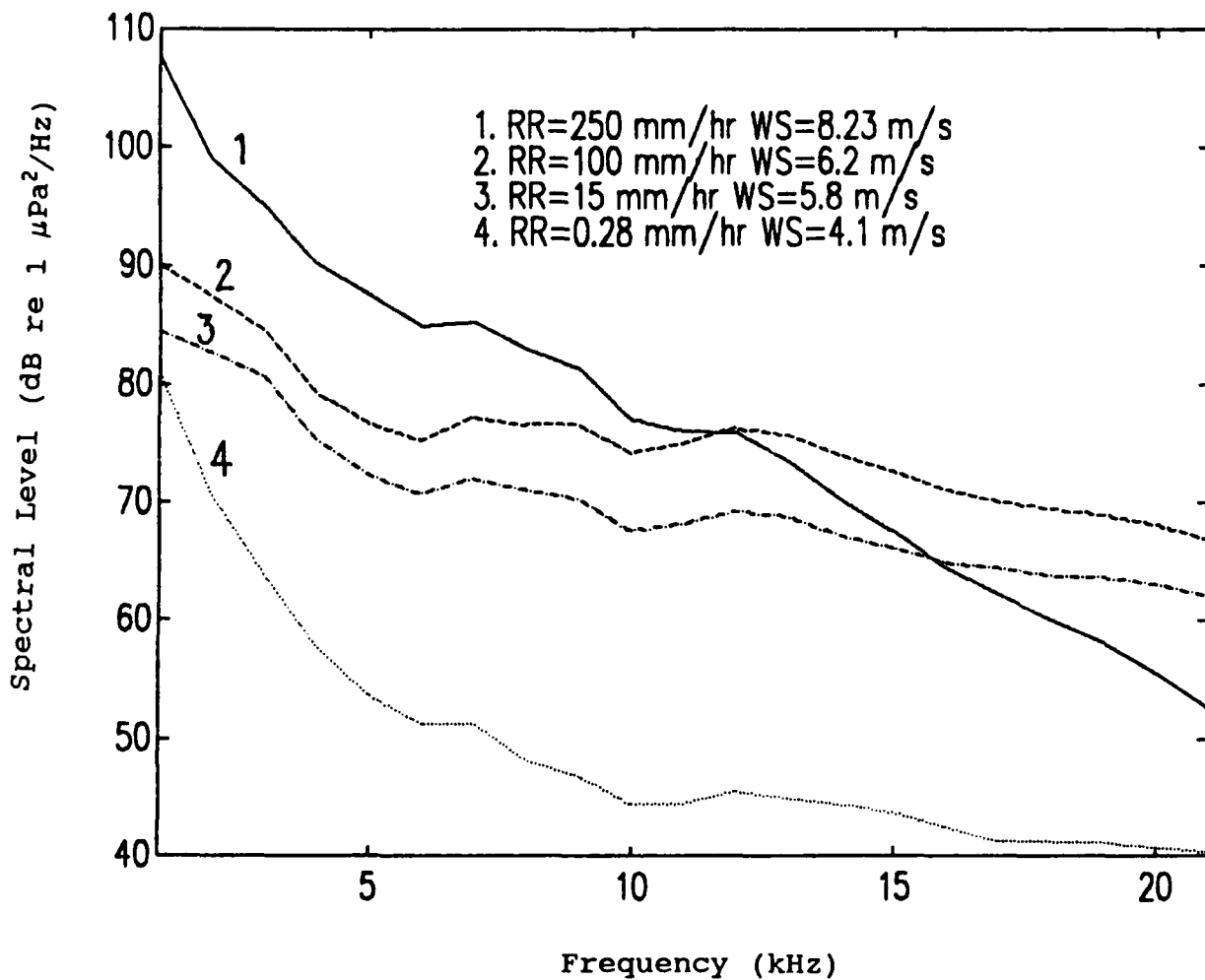


**Figure 30.** The spectral level of four different rainfall rates. Note that as rainfall rate is extremely high (250 mm/hr), same attenuation of the underwater sound at higher frequencies as observed in high wind speed also presents.

observed during extremely heavy rainfall (250 mm/hr) (Figure 30). During high wind conditions this spectral shape has been shown to be due to attenuation of the surface sound because of ambient bubble clouds from breaking waves. Generally for this

phenomenon to be observed, wind speeds are over 10 m/s. In this case, the wind speed is not over 10 m/s and, furthermore, Nystuen (1990), and Tsimplis and Thorpe (1989) suggest that heavy rain will suppress wave breaking. This implies that extremely heavy rain is able to generate an extensive bubble cloud by itself.

**F. CORRELATION COEFFICIENTS FOR AMBIENT SOUND AND RAINFALL RATE**

One of the goals of this paper is to investigate the correlation coefficient between rainfall rate and ambient sound levels over a period of time. For this study, four of the events with relatively constant wind speed were chosen for further analysis. A summary of the environmental parameters: wind speed (WS), wind direction (WD), standard deviation ( $\sigma$ ), and significant wave height etc., is given in Table I.

**Table I.** Environmental conditions of the four different cases with steady winds.

DATE	WS (m/s)	$\sigma_{WS}$	WD (°N)	$\sigma_{WD}$	SIG. WAVE HEIGHT
8/24	3.5	0.4	276	6.6	0.2 m
8/27	1.9	1.0	138	34	0.2 m
8/20	6.3	0.9	312	8.5	0.2 m
8/30	14.7	2.5	050	7.0	0.7 m

The correlation coefficient of the rainfall rate and sound spectral level is defined by:

$$r(i) = \frac{\sum_{t=1}^n (\Phi_t - \bar{\Phi}) (\Psi_{t_i} - \bar{\Psi}_i)}{\left| \sum_{t=1}^n (\Phi_t - \bar{\Phi})^2 \sum_{t=1}^n (\Psi_{t_i} - \bar{\Psi}_i)^2 \right|^{\frac{1}{2}}} \quad (5)$$

Where  $\Phi_t$  is the instantaneous rainfall rate or wind speed field, and  $\Psi_t$  is the instantaneous sound spectral level field. The overbar indicates the average value over the entire time series. The subscript  $i$  refers to the frequency band (1-21 kHz) and the subscript  $t$  refers to the time series.

In the August 24 case, the wind speed was low (3.5 m/s) and the wind direction was nearly constant. The rainfall rate decreased from 14 to 4 mm/hr in the first 90 seconds and then increased back to 13.5 mm/hr during the next 70 seconds and finally back down to 4 mm/hr (Figure 31). The highest correlation is found from 2 to 12 kHz (0.7) and lowest from 14 to 21 kHz (0.5). These values of the correlation coefficient suggest that rain is fairly well correlated with the spectral level. It suggests that low frequencies have better correlation with rainfall rate. This result is consistent with the idea that larger raindrops are better correlated with overall rainfall rate than small raindrops and since larger raindrops produce sound at lower frequencies, the lower frequencies should be better correlated with rainfall rate.

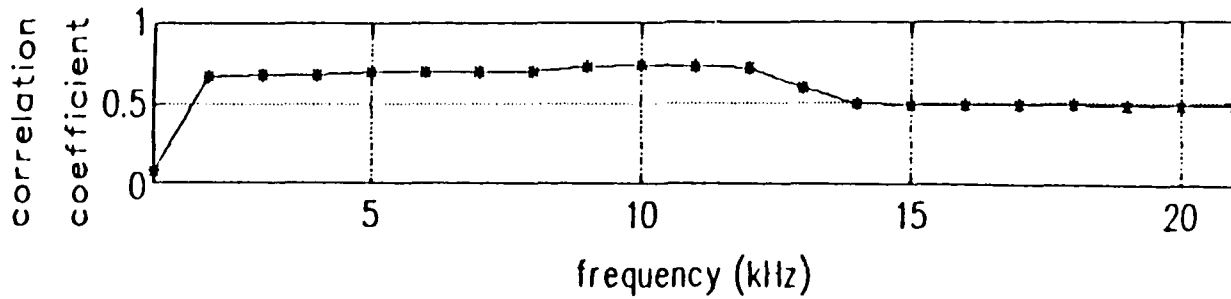
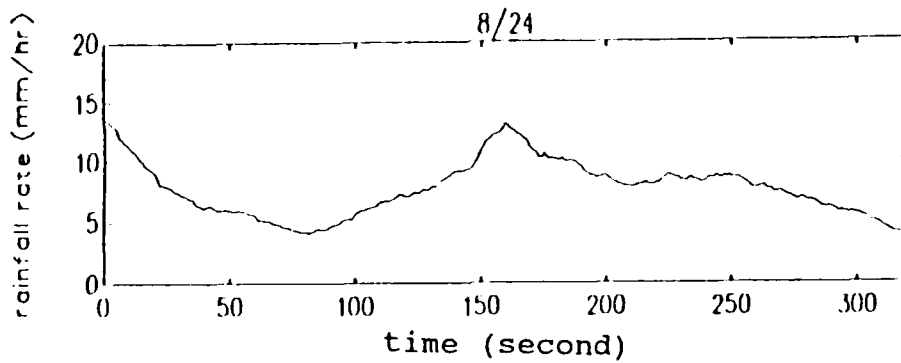
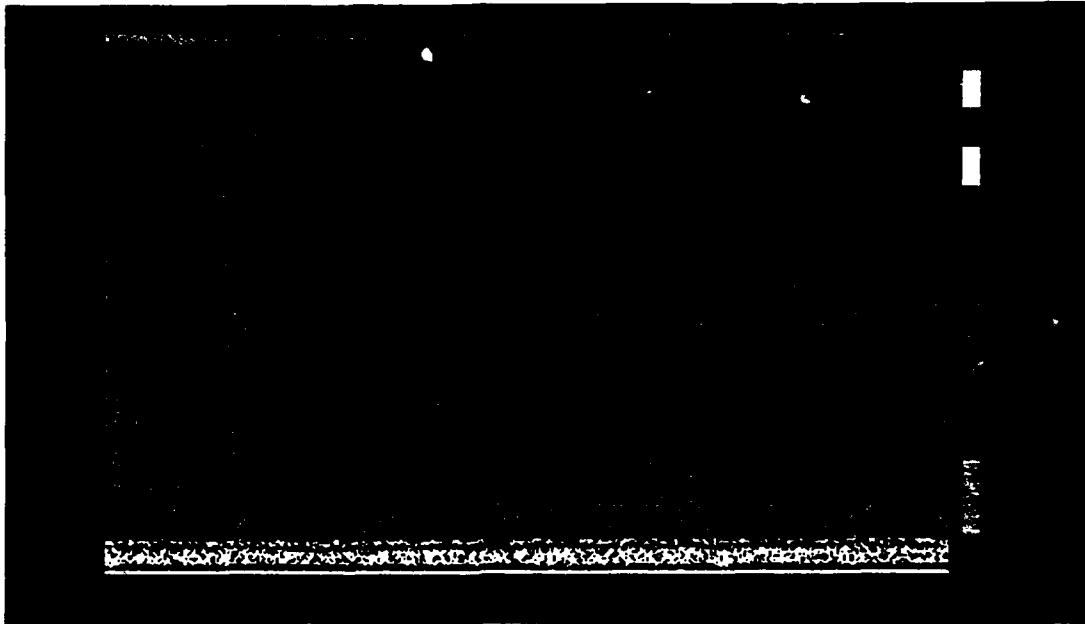


**Figure 31.** Correlation coefficients between rainfall rate and underwater sound spectrum on August 24 from 23:07:00 to 23:12:20. The low correlation at 1 kHz was due to a passing ship.

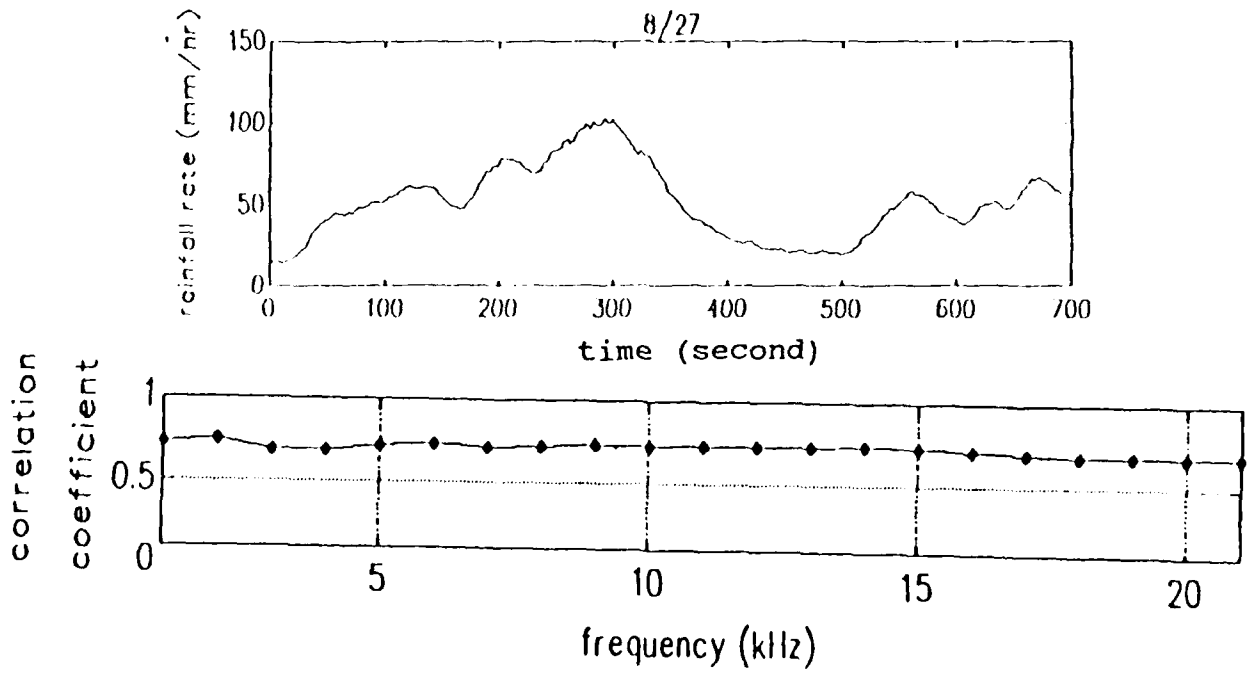
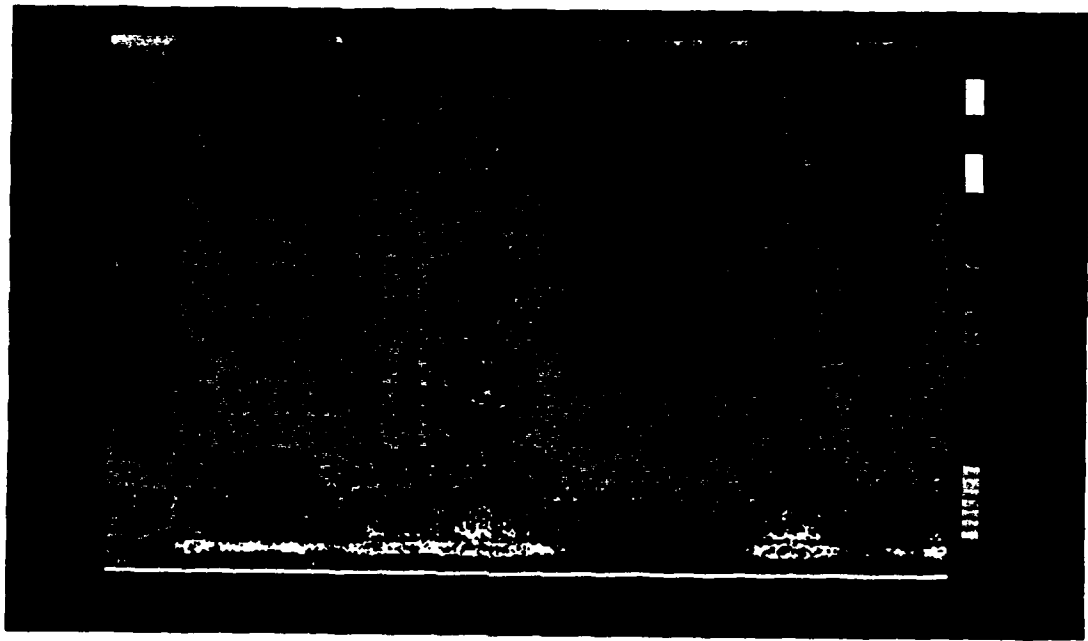
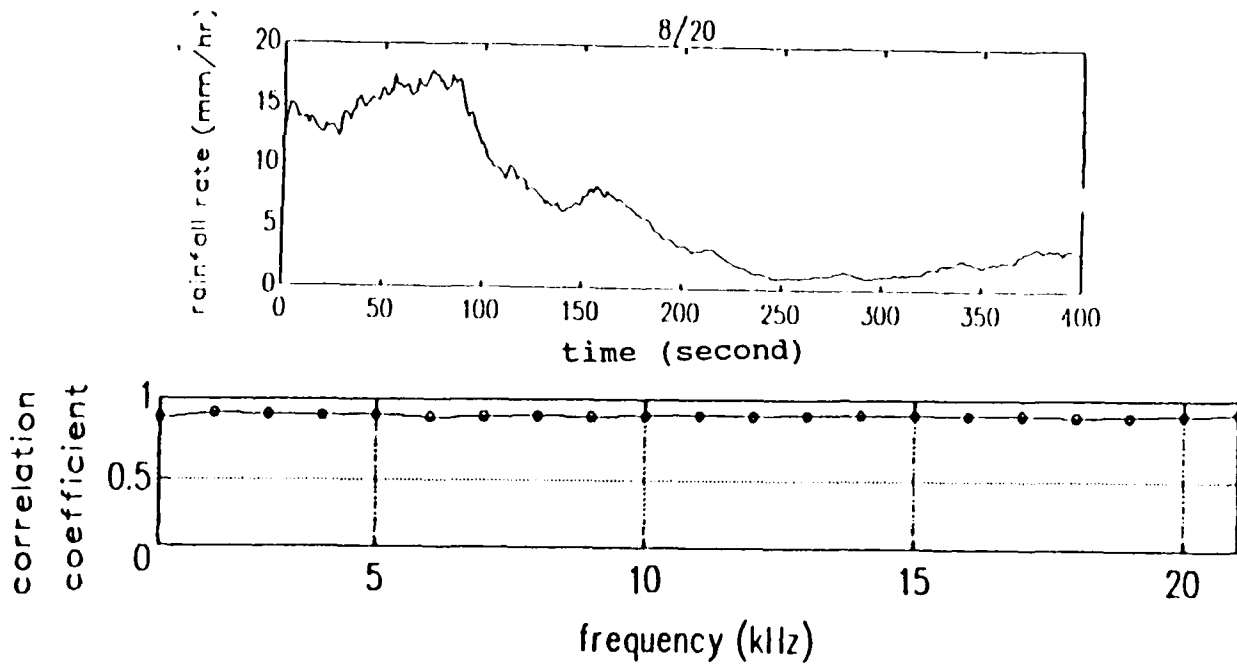
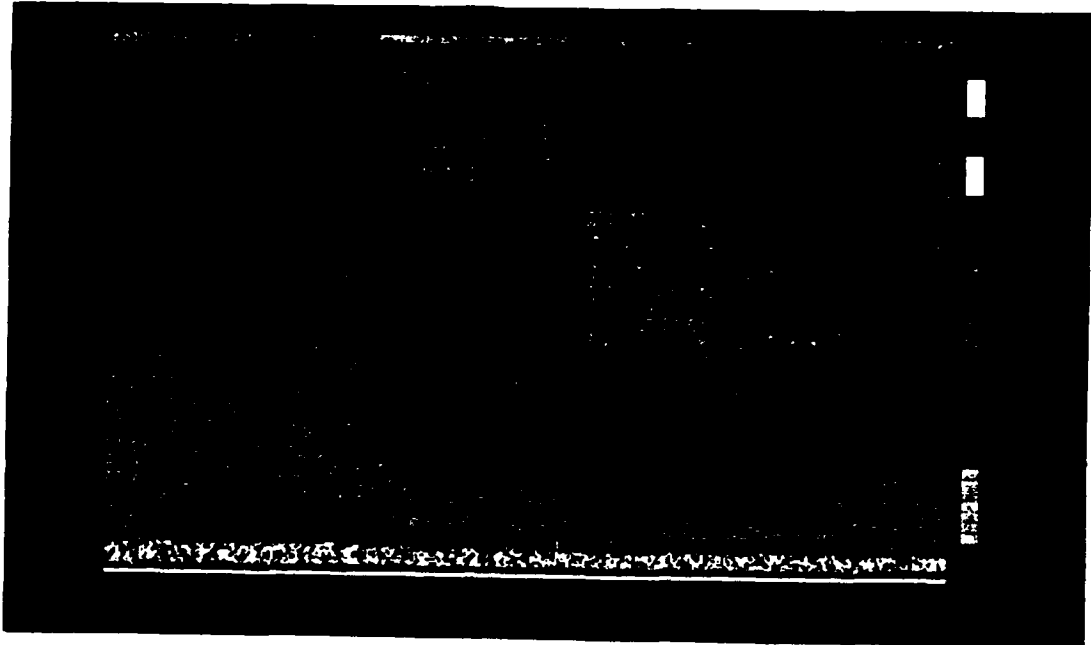


Figure 32. Correlation coefficients between rainfall rate and underwater sound spectrum on August 27 from 07:19:00 to 07:30:40. The best correlation is at 2 kHz for this heavy rain storm.

The second case was recorded on August 27. The wind speed was lower (1.9 m/s) although the wind direction was more variable. The rainfall rate was heavier, varying from 20 to more than 100 mm/hr during 700-second period. Once again, the highest correlation was at 2 kHz (0.74) and the lowest at 20 kHz ((0.69) (Figure 32). Overall, the correlations are higher than Case 1, suggesting that heavier rain is better correlated with underwater sound than light rain.

The third data set (August 20) has uniformly high correlation coefficients. Interestingly, the wind speed was moderately high (6.2 m/s), while rainfall rate varied from 1 to 16 mm/hr during a 400-second period (Figure 33). This case is similar to Case 1 except that the wind speed is now higher. Some effort was made to see if the difference in correlation was due to the wind direction and the physical setup of the hardware. The platform is at 70 meters east (090° N) of the hydrophone. In the Case 1, wind direction is 270° N which caused maximum time lag between hydrophone and rain gauge. In this case, wind direction is 330° N suggesting a minimal time lag. An attempt was made to improve the correlation coefficients in Case 1 by offsetting the rainfall rate data set a few seconds. No improvement was noted. This suggests that the length scale of the rain storm itself is greater than 70 m.

Case 4 was recorded on August 30. Both the averaged wind speed (14.7 m/s) and its standard deviation (2.5) were high



**Figure 33.** Correlation coefficients between rainfall rate and underwater sound spectrum on August 20 from 23:07:00 to 23:13:40. This data set had the highest correlation coefficients of the experiment.

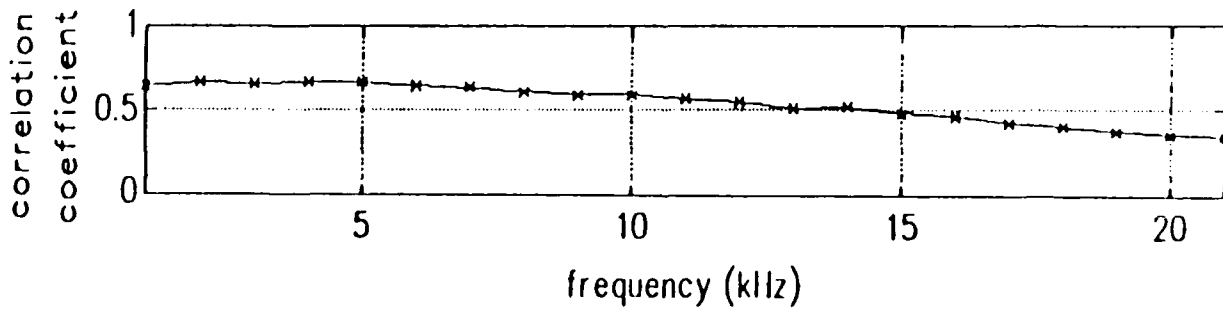
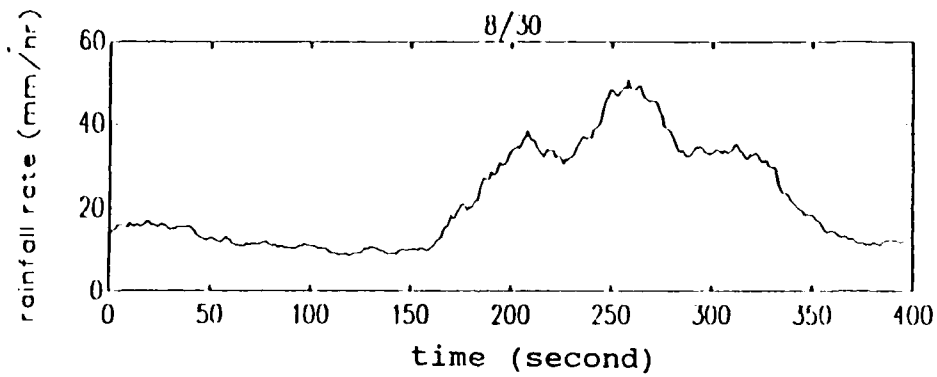
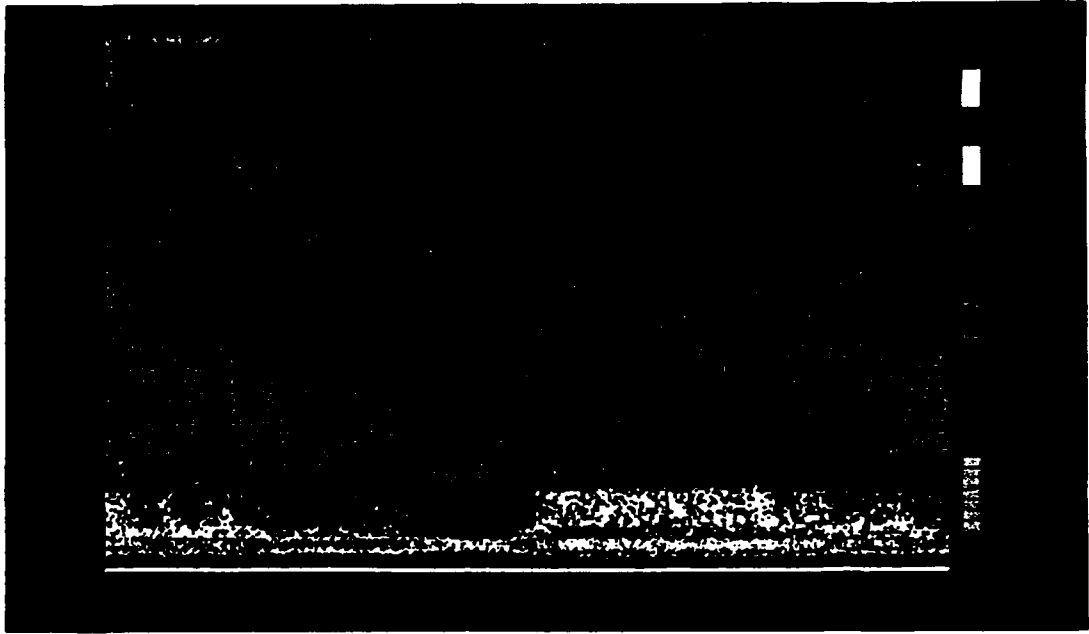


**Figure 34.** Correlation coefficients between rainfall rate and underwater sound spectrum on August 30 from 17:15:50 to 17:22:30. The highest correlation level is 0.68 at 2 and 4 kHz and decreases to 0.34 at 21 kHz.

and the rainfall rate varied from 10 to 50 mm/hr (Figure 34). The highest correlation (0.69) was at low frequency (2 and 4 kHz) and the lowest at 21 kHz (0.34). The poor correlation at higher frequencies suggests bubble cloud attenuation. In this case the wind speed was high enough to expect wide spread wave breaking and subsequent bubble cloud formation (Farmer and Lemon, 1984). Instead of using a high frequency (15 kHz) to measure rain (as suggested by Scrimger et al, 1989), this case suggests that low frequencies will be better for measuring rainfall rate in strong wind conditions.

**Table II.** Summary of correlation coefficients in four different cases.

DATE	Max. $\gamma$	f (kHz)	Min. $\gamma$	f (kHz)	RR (mm/hr)	WS (m/s)	t (s)
8/24	0.70	2	0.50	21	4-14	3.5	320
8/27	0.74	2	0.69	20	20-100	1.8	700
8/20	0.90	all	0.88	6	1-16	6.2	400
8/30	0.69	2	0.34	21	10-50	14.6	400

The results of these four data sets are summarized in Table II.

#### IV. SUMMARY AND DISCUSSION

In this first study of the sound generated underwater by heavy precipitation, several important findings are apparent. The most surprising observation is that the fifteen kilohertz peak which has been reported on and studied extensively during light rain is not present. This peak is suppressed by wind roughening of the ocean surface in the light rain situation (Nystuen, 1990). Apparently the splashes of large raindrops are equally effective at suppressing this peak.

As rainfall rate increases, the underwater sound levels generally increase as previously reported (Scrimger et al., 1989), however the increases are frequency and wind dependent. Under light wind conditions ( $< 1$  m/s), the correlation of rainfall rate with sound level is better at low frequencies ( $< 7$  kHz) than at higher frequencies ( $> 10$  kHz). This result suggests that wind may be affecting the sound generation mechanisms as in the light rain situations (Nystuen, 1990).

At moderate wind speeds ( $\sim 6-8$  m/s), the correlation of rainfall rate and underwater sound is uniformly high, although this is a preliminary finding. Once the wind exceeds 10 m/s, extensive wave breaking is expected and the correlation coefficients show a strong frequency dependence (Figure 34). The lowest correlation is at the higher frequencies ( $> 15$  kHz). This is consistent with the idea that bubble clouds

generated by breaking waves attenuate the surface sound from the rain at higher frequencies. A new finding is that the same effect is observed during extremely heavy rainfall rate (> 200 mm/hr) even when the wind is not over 10 m/s. This implies that extremely heavy rain can be the exclusive generation mechanism of underwater bubble cloud.

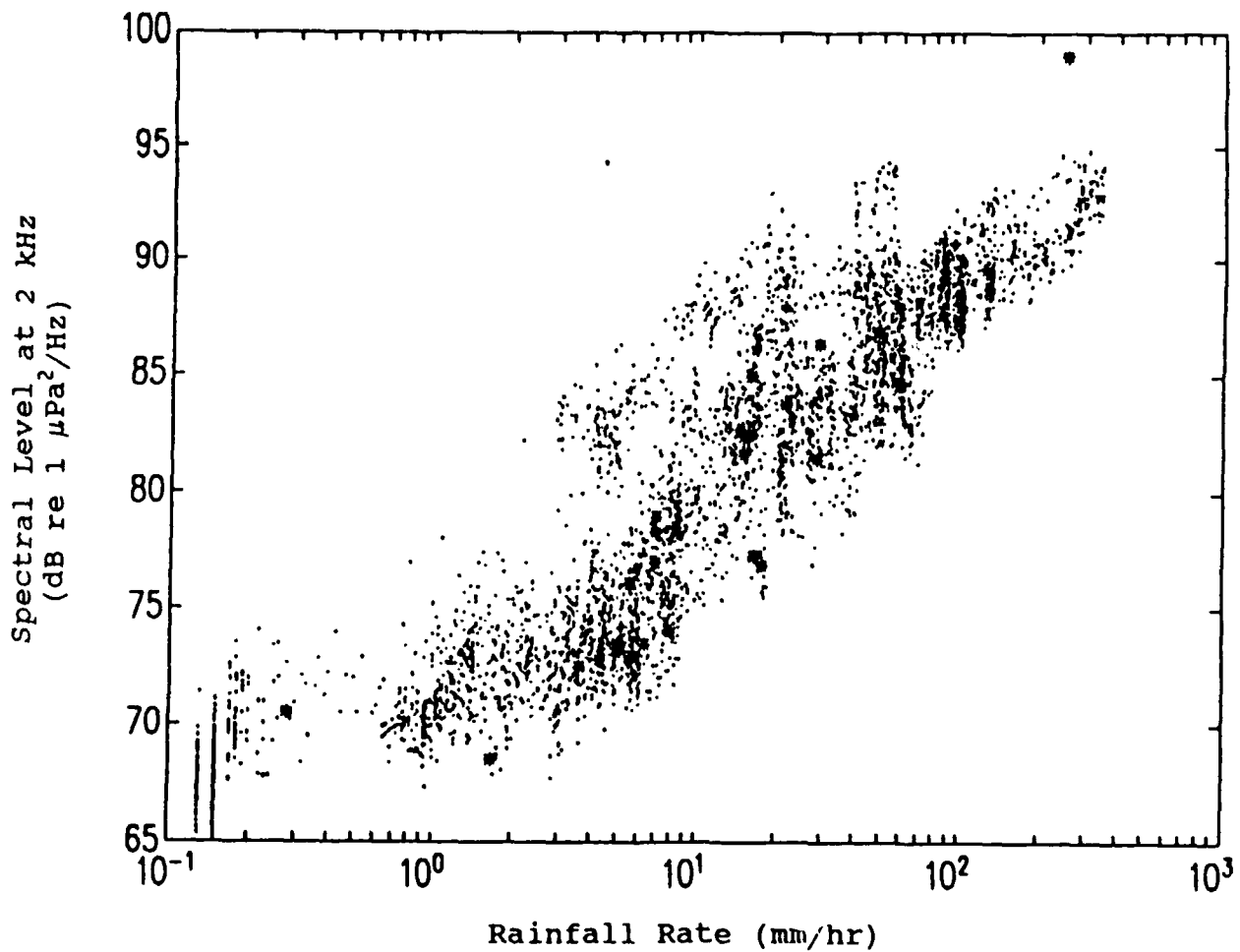


**Figure 35.** Comparison of rainfall rates and the sound spectral levels at 2 kHz. The '·' points are a few averaged values for different rainfall rates under a stable environment (constant wind speed and direction).

Overall the correlation between rainfall rate and underwater sound is better at low frequency ( $< 5$  kHz), unlike the findings of Scrimger et al. (1989). This is because the effects of wind and bubbles are apparently greatest above 10 kHz. Figure 35 shows the comparison of rainfall rate and sound level at 2 kHz (the best overall correlation coefficient) for all of the data collected during Phase 1 of this project. While the scatter is still large, the results are encouraging. Further refinement of the data processing, e.g. multiple correlation regression, and increased understanding of the sound field with rainfall rate, wind stress and bubble populations should eventually lead to a useful technique for inferring rainfall rate from underwater sound measurements.

## V. CONCLUSIONS AND RECOMMENDATIONS

The measurement of rainfall rate by underwater sound is a relatively new idea. If successful, it will be of great use for understanding atmospheric/oceanic heat balance processes, especially for those areas where permanent weather stations are not available. Nine events of various rainfall rate and environmental information were recorded at a coastal ocean location during one month period. The results show that sound at 2 kHz provides the best chance to fulfill this requirement. However, since only 9 data sets were recorded and analyzed, this conclusion is still tentative. The OTP is located in shallow water (15 m) and factors affecting underwater sound transmission such as temperature gradient, salinity, reflection, and seabed generation noise, were not included here. More experiments under different environments are necessary to further understanding of the consequences of local hydrographic effects before future wide spread application can be achieved. If possible, future experiments should attempt to include measurements of the actual drop size distribution in the rain.

#### LIST OF REFERENCES

- Clay C.S. and Medwin H., "Acoustical Oceanography", John Wiley and Sons, New York, 1977.
- Crum L.A. and Pumphrey H.C., "Free Oscillations of Near-surface Bubbles as a Source of the Underwater Noise of Rain", J. Acous. Soc. Am. vol.87, 142-148, 1990.
- Evans D.L., Watts D.R., Halpern D., and Bourassa S., "Oceanic Winds Measured from the Seafloor", J. Geophys. Res. vol.89, No.C3, 3457-3461, 1984.
- Farmer D.M., and Vagle S. "On the Determination of Breaking Surface Wave Distributions Using Ambient Sound", J. Geophys. Res. vol.93, No.C4, 3591-3600, 1988.
- Farmer D.M., and Lemon D.D., "Acoustic Measurement of Wind Speed and Precipitation over a Continental Shelf", J. Geophys. Res. vol.89, No.C3, 3462-3472, 1984.
- Knudsen V.O., Alford R.S., and Emling J.W., "Underwater Ambient Noise", J. Marine Res. 1, 410-429, 1948.
- Kurgen A. "Underwater Sound Radiated by Impacts and Bubbles Created by Raindrops", M.S. Thesis, Naval Postgraduate School, Monterey, CA. 1989.
- Medwin H., and Beaky M.M., "Bubble Sources of the Knudson Sea Noise Spectra", J. Acoust. Soc. Am. vol.86, 1124-1130, 1989.

- Medwin H., Kurgan A., and Nystuen J.A., "Impact and Bubble Sound from Raindrops at Normal and Oblique Incidence", J. Acoust. Soc. Am. 88 (1), 413-418, 1990.
- Nystuen J.A. and Farmer D.M., "The Influence of Wind on the Underwater Sound Generated by Light Rain", J. Acoustic Soc. Am. 82(1) 270-274, 1987.
- Nystuen J.A. and Farmer D.M., "Precipitation in the Canadian Atlantic Storms Program: Measurements of the Acoustic Signature", Atmosphere-Ocean 27 (1) 237-257 1989.
- Nystuen J.A. "A note on the Attenuation of Surface Gravity Waves by Rainfall", J. Geophys. Res. 95, 18353-18355, 1990.
- Nystuen J.A. "An Explanation of the Sound Generated by Light Rain in the Presence of Wind", 1990, to be published in Natural Sources of Underwater Sound, ed. B. R. Kerman, Kluwer Academic Press, 1991.
- Scrimger J.A., Evans D.J., and Yee W., "Underwater Noise due to Rain - Open Ocean Measurements", J. Acoust. Soc. Am. 85, 726-731, 1989.
- Snyder D.E., "Characteristics of Sound Radiation from Large Raindrops", MS Thesis, Naval Postgraduate School, Monterey, CA., 1990.
- Tsimplis M. and Thorpe S.A. "Wave Damping by Rain", Nature 342, 893-895, 1989.
- Vagle S. J., Large W.G., and Farmer D.M., "An Evaluation of the WOTAN Technique of Inferring Oceanic Winds from

Underwater Ambient Sound", J. Atmos. and Oceanic Tech. 7,  
576-595, 1990.

INITIAL DISTRIBUTION LIST

	No. Copies
1. Defense Technical Information Center Cameron Station Alexandria, VA 22304-6145	2
2. Library, Code 52 Naval Postgraduate School Monterey, CA 93943-5002	2
3. Mr. Harry Selsor Code 311, NOARL Stennis Space Center, MS 39529-5004	1
4. Dr. J.A. Nystuen Code OC/NY Naval Postgraduate School Monterey, CA 93943	2
5. Dr. H. Medwin Code Ph/MD Naval Postgraduate School Monterey, CA 93943	2
6. Dr. C. Collins Code OC/CO Naval Postgraduate School Monterey, CA 93943	1

7. Oceanography Research Institute 1  
National Chung-Shan University  
Kaohsiung, Taiwan R.O.C.
8. Oceanography Research Institute 1  
National Taiwan University  
Taipei, Taiwan R.O.C.
9. Oceanography Research Institute 1  
National University of Oceanography  
Keelung, Taiwan R.O.C.
10. Oceanography Division 1  
Operation Department  
Chinese Naval Academy  
Kaohsiung, Taiwan R.O.C.
11. Bureau of Hydrography and Oceanography 1  
Chinese Navy  
Kaohsiung, Taiwan R.O.C.
12. Lcdr. Tan, Chih-Lung 1  
200 Jen-Show St.  
San-Chung, Taipei, Taiwan R.O.C.